TECHNICAL UNIVERSITY OF LIBEREC
Faculty of Mechanical Engineering

Design of a test ejector cooling system.

Master thesis

Study programme:	N2301 – Mechanical Engineering
Study branch:	2302T010 – Machines and Equipment Design
Author:	**Shokry Sobhy Shokry Habashy**
Supervisor:	doc. Ing. Václav Dvořák, Ph.D.

Technical University of Liberec
Faculty of Mechanical Engineering
Academic year: **2017/2018**

DIPLOMA THESIS ASSIGNMENT

(PROJECT, ART WORK, ART PERFORMANCE)

First name and surname: **Shokry Sobhy Shokry Habashy**

Study program: **N2301 Mechanical Engineering**

Identification number: **S16000452**

Specialization: **Machines and Equipment Design**

Topic name: **Design of a test ejector cooling system.**

Assigning department: **Department of Power Engineering Equipment**

R u l e s   f o r   e l a b o r a t i o n :

1. Perform a literature search on ejector cooling.

2. Consider the analytical method of flow calculation in the supersonic ejector.

3. Build a mathematical model of ejector cooling system in a suitable program (MS Excel).

4. Test the mathematical system for various parameters, such as operating temperatures, media.

5. Based on the results, design the basic parameters of the test system.

6. Formulate the conclusions.

7. In the list of used literature, specify at least 10 sources.

Scope of graphic works: **10 pages**

Scope of work report
(scope of dissertation): **50 pages**

Form of dissertation elaboration: **printed**
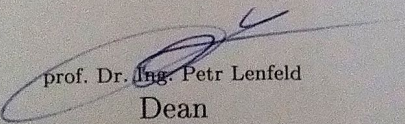
Language of dissertation elaboration: **English**

List of specialized literature:

[1] **J.A. Expósito Carrillo, F.J. Sánchez de La Flor, J.M. Salmerón Lissén,** *Thermodynamic comparison of ejector cooling cycles. Ejector characterization by means of entrainment ratio and compression efficiency.*

[2] **Giorgio Besagni n, Riccardo Mereu, Fabio Inzoli,** *Ejector refrigeration: A comprehensive review.*

[3] **Björn Palm; Per Lundqvist,** *Ejector Cooling System Jianyong Chen.*

[4] **Mohammed Raffe Rahamathullah, Karthick Palani, Thiagarajan Aridass, Prabakaran Venkatakrishnan, Sathiamourthy, Sarangapani Palani,** *A Review on Historical and Present Developments in Ejector Systems.*

[5] **Kamil'Smierciewa, Jerzy Gagana, Dariusz Butrymowicza, Jarosaw Karwackib,** *Experimental investigations of solar driven ejector air-conditioning system.*

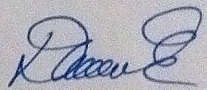[6] **Da-Wen Sun,** *Recent developments in the design theories and applications of ejectors.*

Tutor for dissertation: **doc. Ing. Václav Dvořák, Ph.D.**
Department of Power Engineering Equipment

Date of dissertation assignment: **1 February 2018**

Date of dissertation submission: **1 August 2019**

prof. Dr. Ing. Petr Lenfeld
Dean

doc. Ing. Václav Dvořák, Ph.D.
Head of Department

Liberec, dated: 28 February 2018

Prohlášení

Byl jsem seznámen s tím, že na mou diplomovou práci se plně vztahuje zákon č. 121/2000 Sb., o právu autorském, zejména § 60 – školní dílo.

Beru na vědomí, že Technická univerzita v Liberci (TUL) nezasahuje do mých autorských práv užitím mé diplomové práce pro vnitřní potřebu TUL.

Užiji-li diplomovou práci nebo poskytnu-li licenci k jejímu využití, jsem si vědom povinnosti informovat o této skutečnosti TUL; v tomto případě má TUL právo ode mne požadovat úhradu nákladů, které vynaložila na vytvoření díla, až do jejich skutečné výše.

Diplomovou práci jsem vypracoval samostatně s použitím uvedené literatury a na základě konzultací s vedoucím mé diplomové práce a konzultantem.

Současně čestně prohlašuji, že tištěná verze práce se shoduje s elektronickou verzí, vloženou do IS STAG.

Datum: 14/5/2018

Podpis: Shokry Sobhy Shakry

Acknowledgment

First of all, I owe the Czech Government a big thank you, and the teams involved in candidate's selections of the Czech Government Scholarship for giving me this great chance. Without the scholarship, I wouldn't be writing this thesis. I have experienced a lot in the past two years that substantially changed my perspective on life.

Secondly, I would like to thank my thesis supervisor doc. Ing. Václav Dvořák the head of the Department of Power Engineering Equipment at the Technical University of Liberec. His valuable advice and guidance throughout the course of conducting this thesis helped me a lot in understanding and figuring out solutions to several problems encountered. He has been very patient and understanding to show this paper as it is now.

I would also like to thank doc. Ing. Michal Vojtíšek of the Department of Vehicles and Engines at TUL who helped me so much with his tremendous knowledge in a great way. Also Ing. Jan Kracík of the Department of Power Engineering Equipment at TUL. He has helped me a lot with understanding a lot of things and encouraged me to go through the hard times.

And finally, I would like to thank my family. Since the start of my study here, I set my target is to make them proud. The ride was long and tough, but it was so full of joy and experiences too. I dedicate this work to my mother, Wafaa Yousef. Making you proud is one of my main targets in life.

Shokry Habashy
Author

Table of Contents

SUMMARY

In an attempt to reduce the dependence on fossil fuels, a variety of research initiatives has focused on increasing the efficiency of conventional energy systems.

One such approach is to use waste heat recovery to reclaim energy that is typically lost in the form of dissipative heat. An example of such reclamation is the use of waste heat recovery systems that take the low-temperature heat and deliver cooling in space-conditioning applications. In this work, an ejector-based chiller driven by waste heat will be studied from the system to component to sub-component levels, with a specific focus on the ejector.

The ejector is a passive device used to compress refrigerants in waste heat driven heat pumps without the use of high-grade electricity or wear-prone complex moving parts. With such ejectors, the electrical input for the overall system can be reduced or eliminated entirely under certain conditions, and package sizes can be significantly reduced, allowing for a cooling system that can operate in off-grid, mobile, or remote applications.

The performance of this system, measured typically as a coefficient of performance, is primarily dependent on the performance of the ejector pump. This work uses analytical modeling techniques and makes suggestions for ejector performance improvement. Specifically, forcing the presence of two-phase flow has been suggested as a potential tool for performance enhancement.

This study determines the design parameters for the test system to obtain high COP, also the flexibility of the system to utilize the low-grade energy and get the best outcomes for a reliable ejector cooling system.

INTRODUCTION

As worldwide electricity demand increases and stresses electricity grids to the point of collapse, energy-saving devices have assumed increasing importance for demand-side management.

To reduce the use of high-grade electrical energy, waste heat recovery systems are increasingly considered for applications in air conditioning and refrigeration. The drawback of many waste heat recovery systems is the unfortunate combination of large components and low efficiencies, mostly due to the low waste heat temperatures used.

The ejector-based chiller considered in this work mitigates these issues by offering a solution that is scalable and has operational and mechanical simplicity. It replaces a large and complex compressor component with an ejector pump and does so using a pure, non-toxic refrigerant with low global warming potential.

It obviates the need for lubricating oils, maintenance, or expensive repairs, and allows for waste heat recovery in previously inaccessible applications, including the mobile and/or remote applications that are characteristic of waste heat recovery applications.

The main component of the ejector cooling system is the ejector device itself. This work investigates the ejector on a fundamental level, exploring the nuances of flow inside the ejector in an effort to improve its efficiency and related performance of the ejector cooling system as a whole.

Motivation

Ejector cooling systems have been developed and investigated for their reliability as straightforward devices that can generate refrigeration effect from widely available low-grade heat reservoirs.

The performance coefficient (COP) of a simple ejector cooling system is usually poor, from 0.2 to 0.6. Nevertheless, this depends on the low-grade heat, surrounding, and evaporator temperatures, the performance coefficient also rely majorly on the ejector performance[1].

Also, advancement of the ejector potentially is the highest to improve the coefficient of performance for the whole system. Sadly, deeply investigating of the ejector has been a big challenge due to the complicated flow behavior, to the point that various investigators have described ejector design as more of an artistic work than a scientific one.

However, here in this paper, the ejector performance will be optimized to give reasonable performance parameters considering rational working conditions and to be a very promising solution for the automotive industry and a potential to be utilized instead of the conventional vapor compression cycles.

Ejector nomenclature

Symbol	Unit	Description
A	m^2	Area
a	m/s	Speed of sound
AR		Area ratio between the constant area section and the primary nozzle throat
COP		Coefficient Of Performance
D	m	Diameter
ERS		Ejector Refrigeration systems
fls		Flash tank
GWP		Global Warming Potential
h	J/kg	Enthalpy
m	kg/s	Mass flow rate
M		Mach Number
NXP		Nozzle Exit Position
ODP		Ozone Depletion Potential
p	Pa	Pressure
Q	W	Thermal power Exchanged
s	$J/kg.K$	Specific entropy
$SoERS$		Solar ERS
T	K	Temperature
V	m/s	Velocity
W	W	Power
x		Vapor quality

Greek symbols

Symbol	Unit	Description
ε		Absolute error
η		Isentropic efficiency
ω		Entrainment ratio
Φ		Efficiency due to friction loss
ρ	kg/m^3	Density

Superscripts	Description
*	Critical mode
'	Isentropic state
as	after shock wave
c	exit of the ejector
co	backflow mode

$comp$	compressor
$cond$	condenser
$Conf$	Configuration
ej	Ejector
e	evaporator
exp	Experimental
fls	Flash tank
g	Generator
In	Inlet
m	Mixed
$Mech$	Mechanical
Num	Numerical
out	outlet
p	primary inlet
$p1$	Primary nozzle exit
py	primary flow at sec.flow choking
s	Secondary inlet
sy	secondary flow at choking
sub	sub-cooling
sup	Super heating
t	Throttle

Pump nomenclature

Symbol	Unit	Description
Q_p	m^3/s	Flow rate
p	$Pascal$	Pump pressure
η_{pump}		Pump efficiency
Pump power	kW	Power

Heat exchanger nomenclature

Symbol	Unit	Description
P	kW	Thermal power
δt	K	temperature difference between outlet and inlet on one side
k	$W/m^2 K$	heat transfer coefficient
$LMTD$	K	Log. Mean temperature difference
$T1$	K	Hot-side inlet Temp.
$T2$	K	Hot-side outlet Temp.
$T3$	K	Cold-side Inlet Temp.
$T4$	K	Cold-side Outlet Temp.

1.1. EJECTOR COOLING SYSTEMS

The ejector based cooling cycles are powered by the low-grade heat, that uses excess heat dissipated for refrigeration in automotive to decrease the demand on fossil fuels usage and instead utilizes solar energy for air conditioning: it's required to cool down some zone when the sun shines.

The concept of the ejector existed through the last 100 years. Because it can produce negative pressure and after building up the pressure through the subsonic diffuser, it's a good potential to be used in the cooling systems especially when the low-grade heat is easily provided through some applications such as automotive, solar and, manufacturing and industrial facilities etc. [2].

Nevertheless, the environmentally friendly working fluids are capable of being utilized, that reduces ozone depletion and simply emphasize the environment-friendly concept achieving major energy saving.

The ejector based chillers offer a feasible opportunity to obtain energy savings and clean environment, simple structure, building, and operation with minimum maintenance.

Nonetheless, there at the moment, there is no ejector cooling system for commercial usage in markets because of the low $COP_{thermal}$, while good $COP_{mechanical}$ [2].

1.2. Ejector working principles and cycles Configuration

The operating concept mainly depends on this potential of high-pressure conversion of the primary flow into movement or velocity energy via the motive nozzle. As shown in Fig. 1, the device consists of a main (primary or motive) nozzle that accelerates the highly pressurized working fluid.

Because of the effect of the Venturi, the motive flow drives the induced flow at the secondary nozzle. In the mixture part both fluids merge, the pressure

increases due to a shockwave and then the mixture decelerates, also through the diffuser.
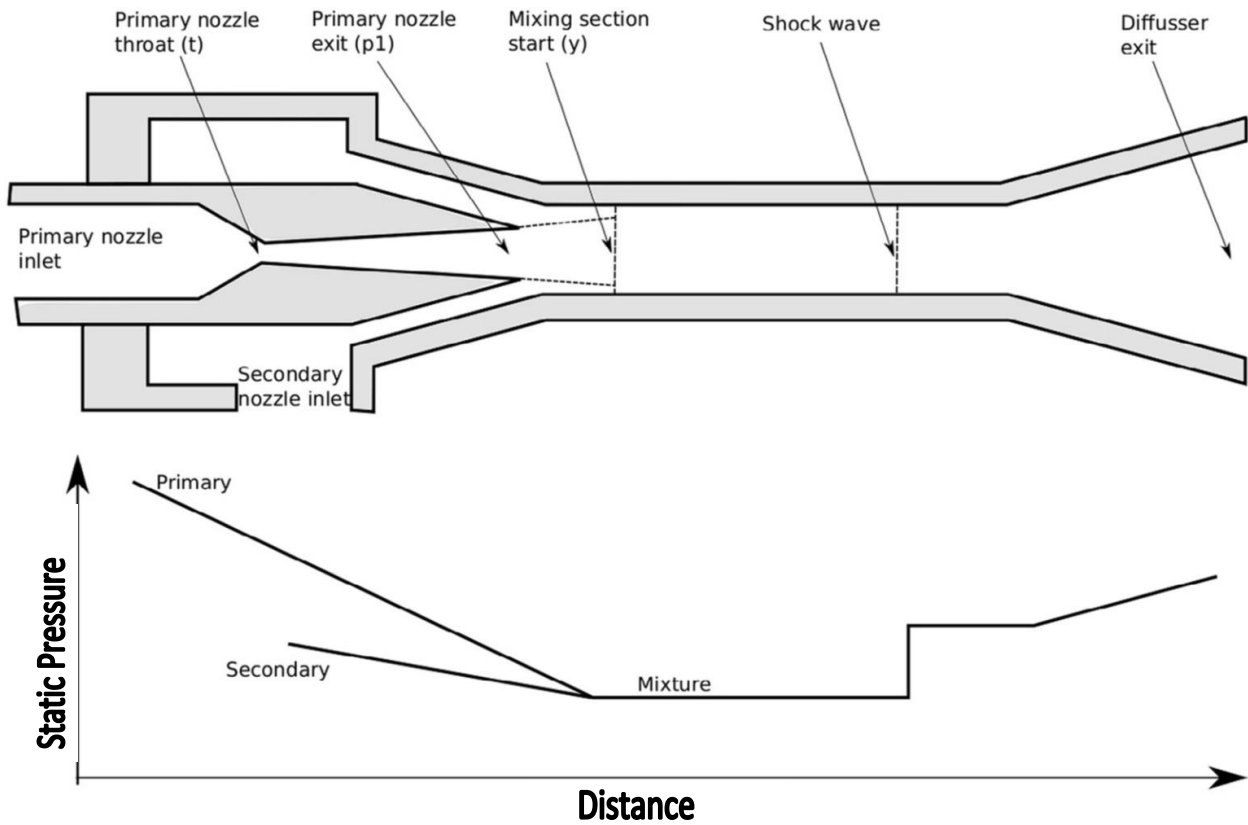
Figure 1-Geometry and pressure evolution in ejector $[4]$.

The biggest benefits of ejector are, as was mentioned by Chen et al. (2013b) [3], the simple structure and fitting, doesn't require much maintenance besides the recovery and usage of the low-grade energy. But, the off-design performance is not that great.

There are three different probabilities of performance could occur regarding the back pressure "p_c", as a result of the involved flows in the ejector (Pianthong et al., 2007) [4].

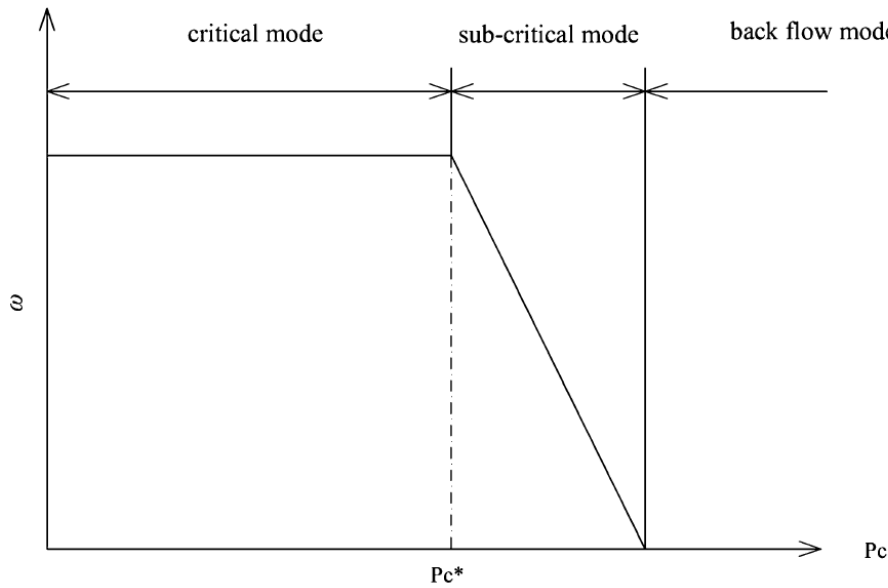Figure 2-Operational modes of ejector $[4]$.

The critical pressure *Pc** is usually explained as the back pressure that entrainment ratio (secondary to primary mass flow rate ratio) ω stays constant; Figure 2.

When the back pressure is lower than *Pc**, the secondary and primary flows are under choking effect; therefore, the mass flow rate is highest. That behavior usually is known as the critical point. Higher pressure than *Pc**, there is no more chocking in the secondary nozzle, although the primary is choked yet, the *Pc* increases when the entrainment ratio decreases.

When the *Pc* keeps getting higher, the primary nozzle then stops being choked therefore, the entrainment ratio reduces and at the end it's possible for the flow to go in the opposite direction.

It was mentioned in Huang and Chang [3], the critical back pressure increases also the primary pressure, however, the critical entrainment ratio decreases significantly.
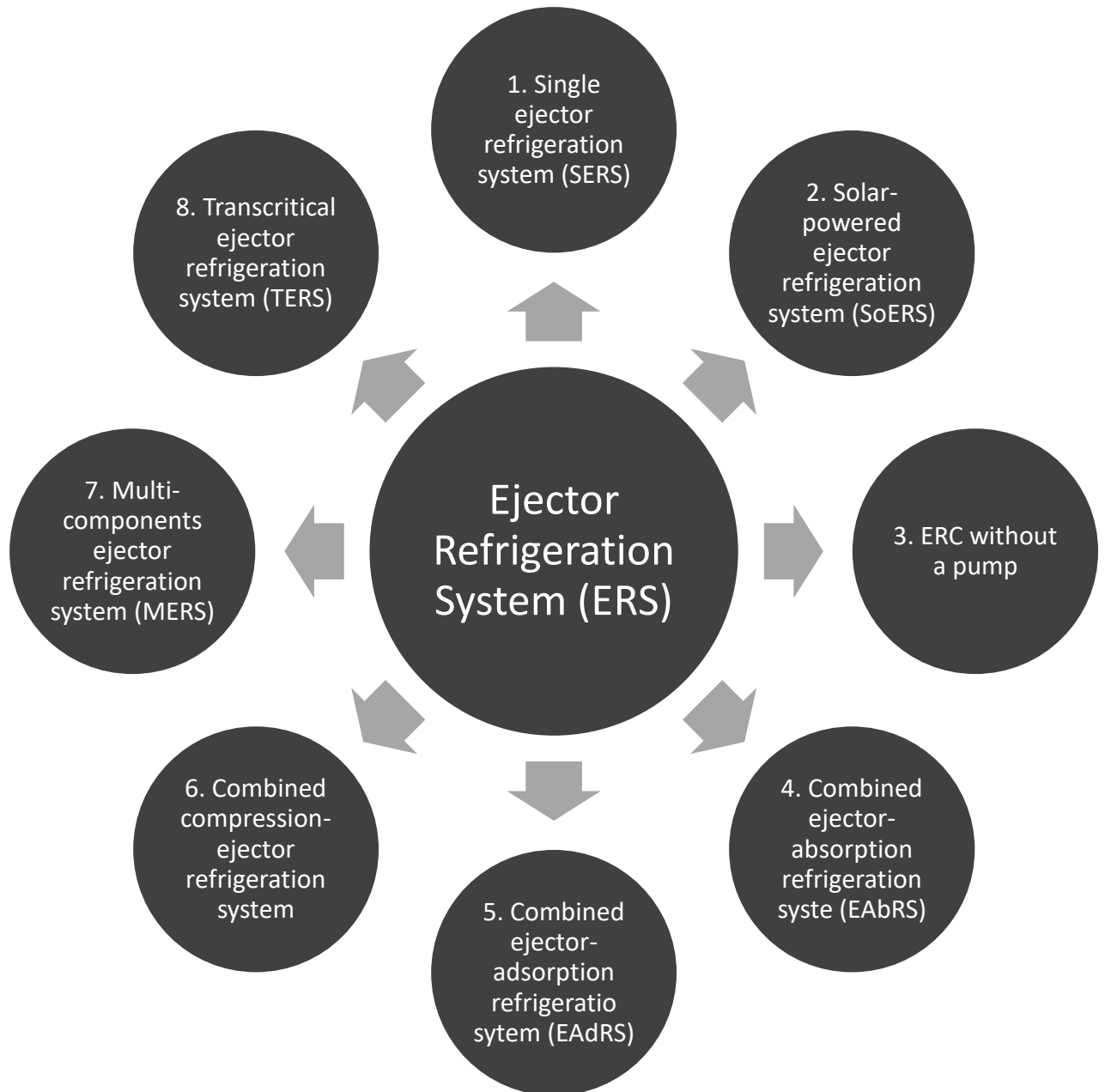
1.3.   Ejector cooling classifications:

Figure 3-Ejector classification [5]

Table 1 Ejector types and classifications [5]

Parameters	Condition			Classification	Remarks
Nozzle position	Inside suction chamber			CPM ejector	Better performance if compared with CAM ejector
	Inside constant-area section			CAM ejector	–
Nozzle design	Convergent			Subsonic ejector	–
	Convergent-divergent			Supersonic ejector	–
Number of phases	*Primary flow*	*Secondary flow*	*Exit flow*		
	Vapor	Vapor	Vapor	Vapor jet ejector	Possible two-phase flow
					Possible shock waves
	Liquid	Liquid	Liquid	Liquid jet ejector	No shock waves, single-phase flow only
	Vapor	Liquid	Liquid	Condensing ejector	Two-phase flow with primary flow condensation
					Strong shock waves
	Liquid	Vapor	Two-phase	Two-phase ejector	Two-phase flow
					Shock waves possible

The ejector usually categorized either by the position of the nozzle, design of nozzle or the working phases, as was shown in Table1. Giorgio Besagni [5].

Corresponding to the investigated works by the researchers, there are about seven configurations we're interested in reviewing, besides the traditional reversed Rankine cycle[6].

Principle configurations in Figures. 4 to 9. The majority of other cycle topologies can be combined with them.
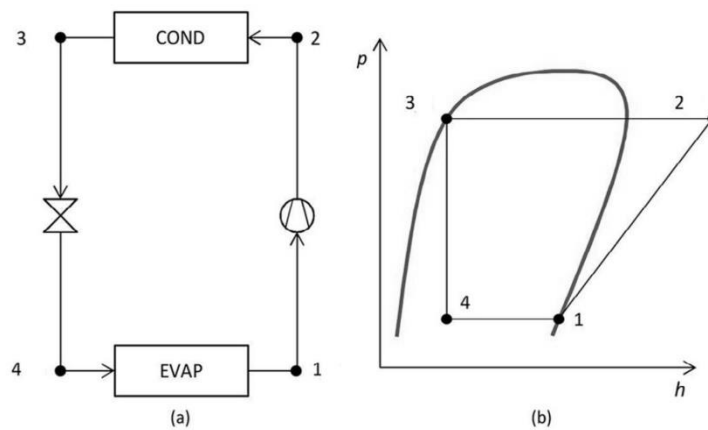

Figure 4-Vapour compression cycle (Conf. 0). [4]

The classic vapor compression cycle consists of a compressor to raise the pressure, a condenser to liquefy the hot high-pressure gas, expansion valve to drop the pressure and the evaporator to absorb the heat from the cooled space. Topology no. 1a, Figure 5, can be redesigned by exchanging the ejector and
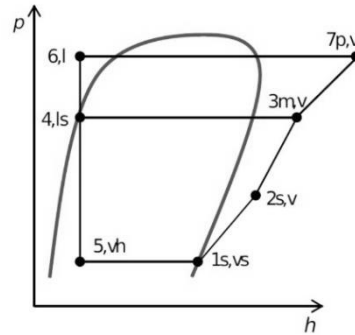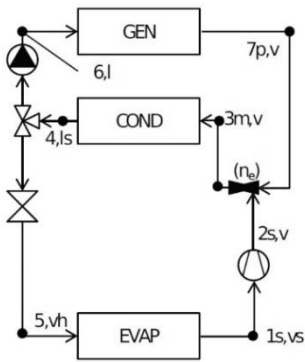
Figure 5 –Ejector cycle with compressor (1a). [4]   Figure 6 – Multi-stage compression cycle (2a). [4]
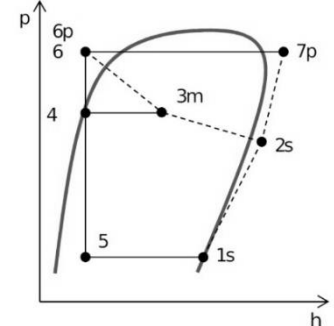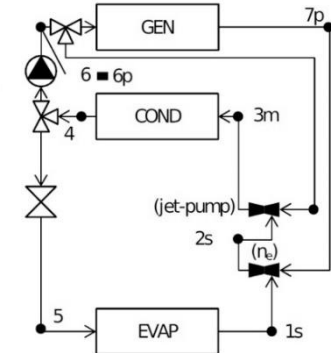
compressor to get configuration 1b [7]. configuration 2a Yu et al. [7], Figure.6, can be changed by exchanging the jet-pump (ejector that uses the liquid as a motive fluid) with an ejector, these two topologies use primary fluid from point 7, to get configuration 2b, Zeng et al.

The 3rd cycle layout in figure 7, is dual-phase uses a jet pump (high-pressure liquid is the motive fluid) for expansion [8, 9].
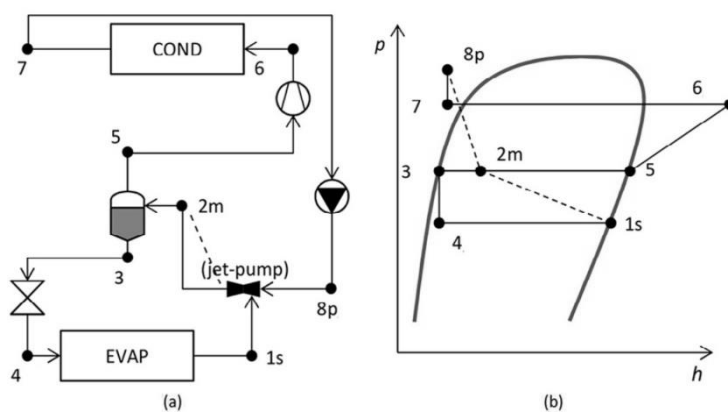
Figure 7 – Jet pump cycle. [4]

The researchers of this topic suggested installing an extra pump at the discharge of the condenser heat exchanger like the most general configuration of the jet pump cycle.

Nevertheless, it was clear in most cases that the pump isn't needed [4].

Layout 4a in figure 8 is a complex cycle layout which makes it easy to use various working fluids in both the low and high-pressure cycles despite using only one working fluid in this investigation.
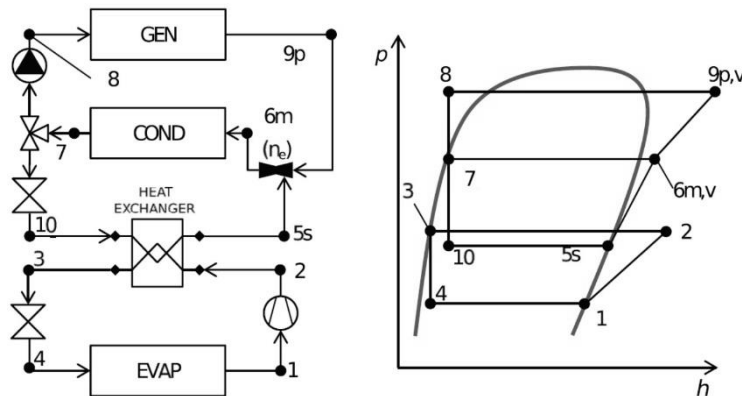
Figure 8 – Cascade cycle (4a). [4]

This sort of arrangement is normally utilized for cooling at low temperature utilizing working fluids in an alternate scope of temperatures, be that as it may; it has been incorporated into this investigation to demonstrate its potential improving performance.

While working fluid is utilized, the heat exchanger can be supplanted by a flash tank where the gas and liquid are isolated, utilizing the gas as the secondary stream of the ejector and the fluid is expanding in the valve to the evaporator [4].
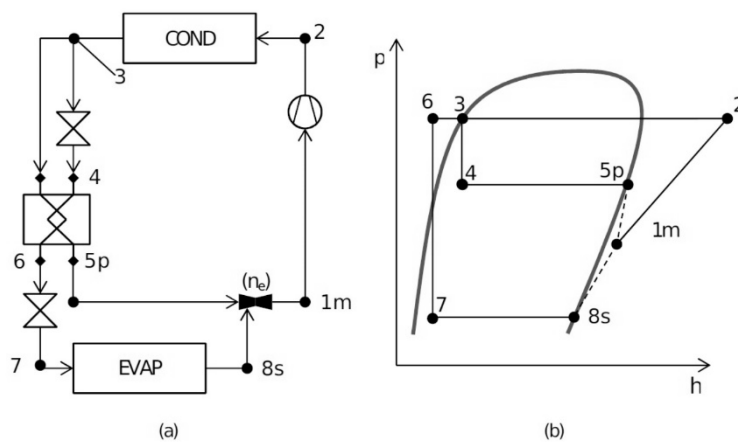
Figure 9 – Booster with economizer (5a). [4]

Layout.5a is an ejector boosting cycle with an economizer that is dedicated to pumping up the subcooling (cooling the liquid). The vapor generated at the economizer discharge is utilized at the primary intake of the ejector.

A similar typology of the cycle was proposed by Yu et al. (2008)[7] for using a mixture of refrigerants with a different boiling temperature range, this cycle is a so-called auto-cascade cycle. A phase separator is placed after the condenser in order to split the mixture of refrigerants.

In recent years, coupled Rankine and So ERC systems have been proposed, and they can be energy-efficient, reliable and flexible in operation. However, efforts are needed to optimize these cycles and for developing model sable to consider transient phenomena in every component of the cycle [5].

Table 2 provides a general overview of solar-driven ERS performance and operating conditions. Another proposal, different from the previous ones and not reported above, is the coupled photovoltaic-heat pump systems for water heating. This system was proposed for and industry application.

The system may suffer from control issues (i.e., difficulty of maintaining the vacuum required by the low evaporation temperature) and further studies are required.

Table 2 Conditions and performance of operation (T) theoretical and (E) experimental study [4].

	Working fluid	Generator temperature [°C]	Evaporator temperature [°C]	Condenser temperature [°C]	$COP_{ejector}$ [–]	CC [kW]
E	R11, R12, R113, R114, R717, H_2O	60–100	10–18	40–50	0.42 (max)	0.21
T	R141b	80–120	−6–8	30–36	0.20–0.50	10.5
T	R600	85–125	5–15	37	0.20–0.40	5
T	R134a	82–92	−10–0	32–40	0.035–0.20	–
T	R123	85	12	30	0.20	3.7
T	R134a R141b R142b R152a R245fa R290 R600 R717	90	15	35	0.30–0.41	–
E	H_2O	84–96	6–13	21–38	0.17–0.32	5
E	R600a	50–64	4–7	22–32	0.15–0.20	2
T	R245fa	90–110	12–20	35–40	0.2–0.55	10.5
T	R142b	105	−10	30	0.34	2
T	R141b	80	8	32	0.39	10.5
T	R600a	70–120	5–15	$T_{amb}+5$	0.35–0.48	3.5
T	H_2O	90–110	5–15	30–40	0.10–0.55	5
T	R134a	85	8	$T_{amb}+\Delta T$	0.30–0.53	6
T	R141b	80–110	2–14	20–40	1.5 (max)	3.5
E	H_2O	110–135	2.5–10	21–30	0.5 (max)	–
T	H_2O	150	−11 to −3	24–30	$\eta_l=0.148$[a]	–
T	R1234yf, R1234ze, R290, R600, R600a, R601, R744	150	12	50	$\eta_l=0.151$[a]	–
E	R600a	83	9	21–29	0.2–0.58	–
T	R717 R134a R600 R600a R141b R152a R290 R123	80–100	8–12	28–40	0.59–0.67	
T	R134a	26 bar	8	30	0.52–0.547	7
T	R141	85	35	8	0.1–0.7[b]	5

The numbers shown here in the table indicates to conditions range regarding every study.

1.4. Ejector cooling system without a pump

The pump does not represent a major increase in investment or power usage (i.e., in <u>Pridasawas W, Lundqvist P.</u> [10] the pump demand of electricity consumption is about 0.18% of the received energy from the sun [5]. But, the pump demands extra maintenance than the rest of components due to being the only device with moving parts in the ERS. Therefore, to eliminate the pump, various ways were invented:

- Gravitational-rotational ejector cooling cycle.
- Bi-ejector cooling cycle.
- Ejector cooling system with thermal pumping effect.
- Heat pipe-ejector cooling cycle.

Through these methods, the ejector cooling cycles obtain additional advantages, like the expected probability of prolonged lifespan requiring minimum maintenance, great reliability and zero moving parts.

Therefore, a lot of research and development engineers have tried to find different ways to avoid those disadvantages.

1.4.1. Gravitational and rotational ejector cooling system

The configuration of a gravitational ejector cooling system is shown in Figure 10 Kasperski suggested a gravitational ejector [7].
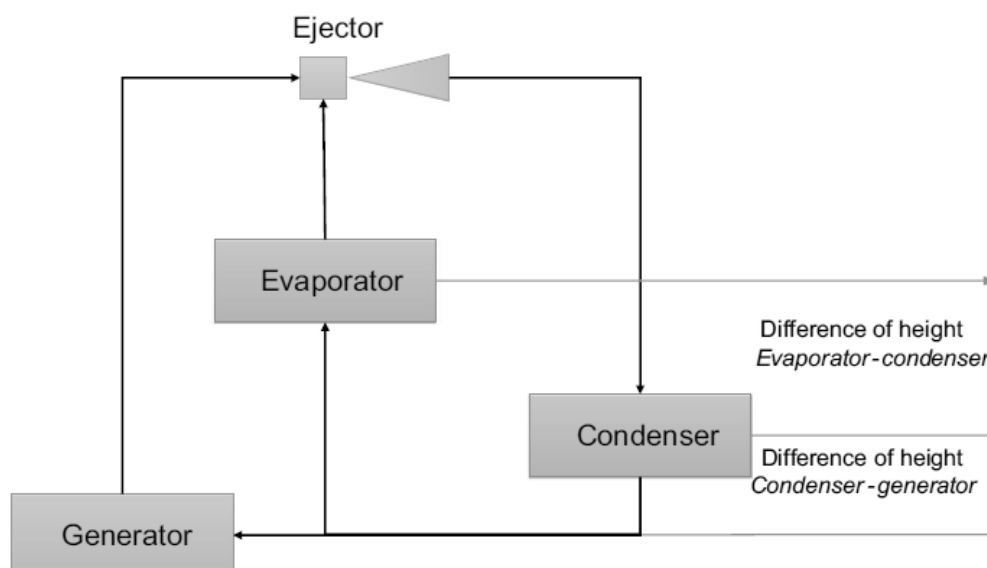
Figure 10 –Gravitational ERS. [5]

Regarding this layout, the heat exchangers supposed to be positioned on different heights, resulting in the pressure differences required among them.

The highest pressure usually in the vapor generator and the least pressure in the evaporator. The self-regulation complicated mechanisms are in each heat exchangers condenser, generator, and evaporator.

The vertical differences requirement in heights is the major drawback of the system (it depends on temperature differences and working fluid) and pipes total length (that results in heat loss and friction loss).

At T_g (generator temp.) = 80 °C, T_e (evaporator temp.) = 15 °C and T_{cond} (condenser temp.) = 35 °C, the COP (coefficient of performance) is 0.16. The concept of the gravitational ejector was developed by the same researcher to a rotational ejector Fig. 11, which decreases the total bulk of the gravitational system and the refrigerant (roughly1000 revolutions per minute) [5].
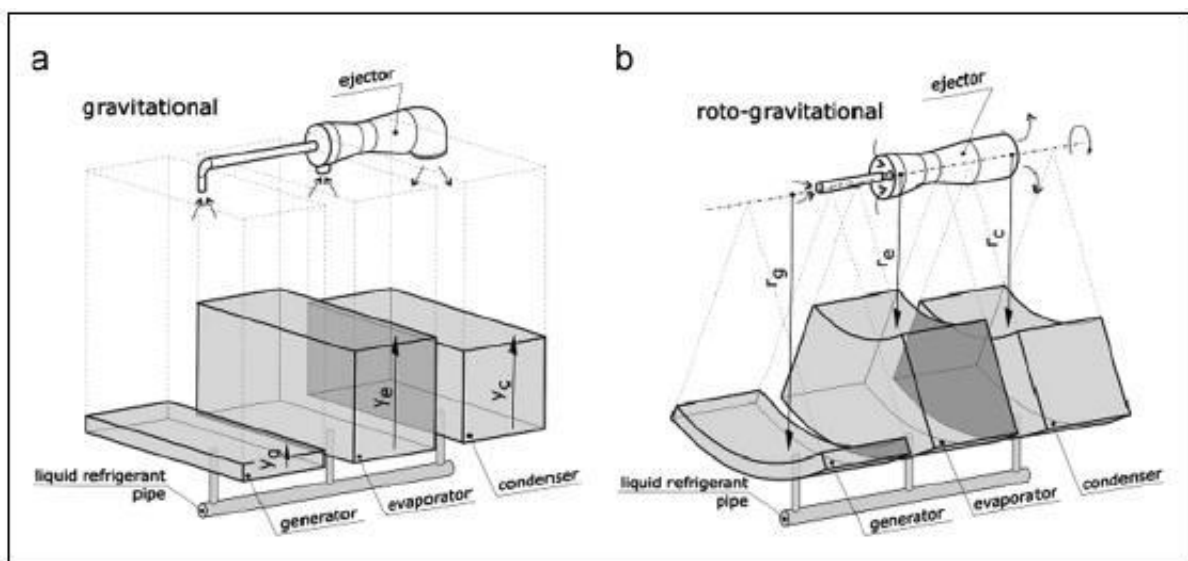
Figure 11–Liquid working fluids Levels in Gravitational (a) and Rotational-Gravitational (b) Ejector cooling systems [7].

It has quite similar performance as the gravitational ejector: COP = 0.16 (T_g = 90 °C, T_e=15 °C, T_{cond}=35 °C). A solar-powered ejector system was investigated built on the natural convection by Nguyen et al.: liquid circulation is driven by gravity from the condenser to the generator (system height exceeds 7.5m).

The proposed cycle for HVAC usage uses water as working fluid (the refrigerant). In the winter season, this system is able to be used for heating and was assessed and built in an office building in the UK.

The refrigeration effect of the prototype model was about 7 kW and reached a COP of 0.3. The payback time for the investment was 33 years [5].

Besides to the economic concerns, this system contains different critical points, especially, the huge thermal inertia, that slow down the starting and shut-down processes. Also, the usage of the extra burner is needed through an off-design operation for more heating as well as to eliminate thermal transients.

1.4.2. **Bi-Ejector cooling System**

In the bi-ejector cooling system, an extra ejector, instead of the pump, pumps the condensed liquid to the generator. Hence, the ejector is a vapor/liquid ejector. The configuration of a bi-ejector cooling system is presented in Fig. 12.

In case of ideal operation, this system does not need electricity, that's why it's more attractive. Shen et al. did numerical studies for this layout, and the results obtained that the cycle COP is majorly affected by ω for the tested working fluids (R123, R134a, R502, and R717, water, etc.) [5].

The highest COP obtained was 0.26 with R717. But, Wang and Shen analyzed a solar version using R123. The results clarified that increasing generator temperature ω of the two ejectors results in different behaviors: one increases and the other decreases.
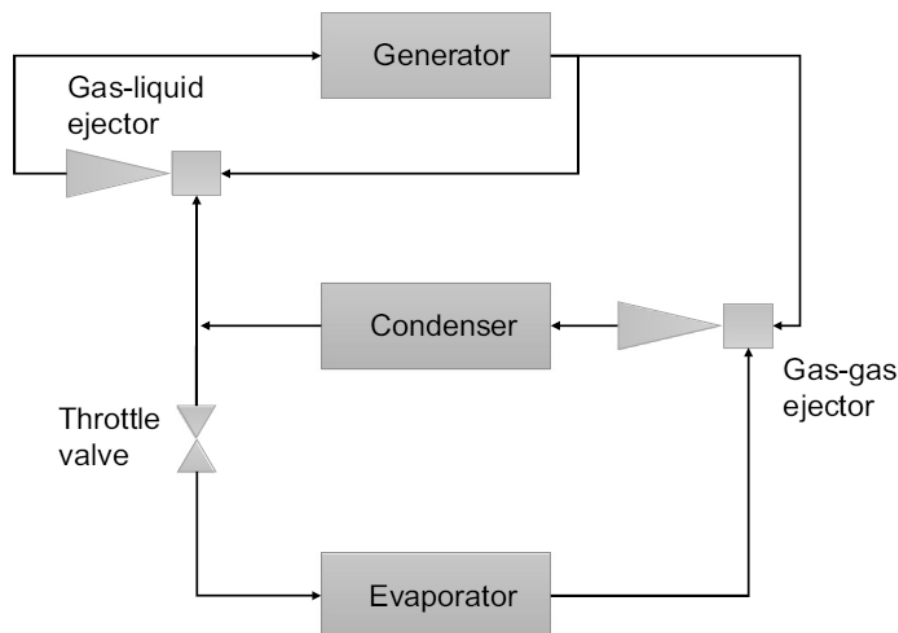
Figure 12 – Bi-ejector cooling system without pump by Wang and Shen (2009) [5].

Hence, the overall optimum thermal efficiency for this cycle is 0.13 (T_g = 105 °C, T_e = 10 °C, T_{cond}= 35 °C). In case of increasing T_c, the ω of both ejectors and the whole system efficiency will be decreased [5].

1.4.3. Ejector cooling system using thermal pumping effect

Ejector cooling system using thermal pumping effect may be workless-generator-feeding or multi-function generator.

Huang et al. proposed a multifunction generator: the system contains one more generator, both of them composed by a boiler and an evacuation chamber. The liquid is heated by the boiler, and the cooling effect is provided by the evacuation chamber.

The system consists of many components, that results in a usage of thermal energy. The experiment results reported COP = 0.22 (T_g = 90 °C, T_e = 8.2 °C, T_{cond} = 32.4 °C), regardless the extra heat requirements for the multi-function generator operation. Considering the extra heat requirements, the overall COP is decreased to be 0.19.

To change R141b, Wang et al. investigated the ejector system using R365 MFC (Mixed Flow Cascaded). It resulted in a conclusion R365 MFC can be used instead of R141b keeping the performance of the system.

At T_g = 90 °C, COP $_{ejector}$ = 0.182–0.371, the total COP = 0.137 to 0.298, and cooling capacity= 0.56 kW to 1.20 kW for T_e = 6.7 to 21.3 °C. Sri Sastra et al. introduced a workless-generator-feeding, using R141b, without a pump [5].

1.4.4. Heat pipe-ejector cooling system

The combination of an ejector with the heat pipe will result in the high-performance compact system, without the need of the work of pump. Solar energy or hybrid sources can be utilized and so decrease electricity demand and also fossil fuel usage.

The elementary cycle of the heat pipe-ejector cooling system appears in Fig. 13. The framework comprises a heat pipe, ejector, evaporator and thermostatic expansion valve. The low grad energy is added to in the generator segment. At that point, the refrigerant dissipates and courses through the motive nozzle of the ejector.
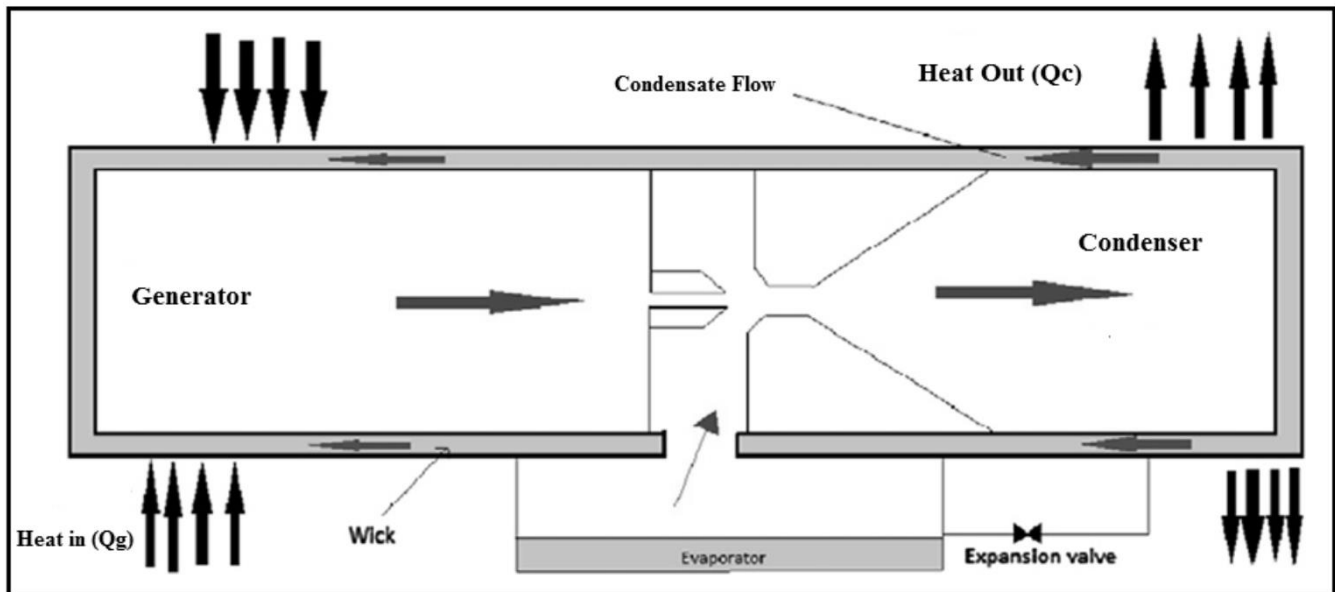
Figure 13 – Heat Pipe - Ejector cooling system configuration [7].

Consequently, it expands and decreases the evaporator pressure. In this way, the cooling cycle can be closed. At the condenser, a portion of the refrigerant back to the generator by the wicked activity, while the rest was expanded to the evaporator through the expansion valve.

Not at all like other reversed Rankine cycle, which is driven by mainly electric power generated by huge plants, the heat pipe-ejector cooling systems do not need any electric power, Ziapour et al. investigated an energy and exergy examination in light of the 1st and 2nd laws of thermodynamics [5].
The results of the simulation were analyzed with accessible experimental data for ejector cooling system. The COP of methanol was greater than that of the rest of fluids, approximately 0.7. In general, COP~0.5 is possible utilizing low-grade thermal energy working parameters [5].

1.4.5. **Ejector-absorption combined cooling cycle**

Absorption cycles are able to utilize low-grade thermal energy, i.e. the Sun power, waste heat or the fuel burning exhaust. Nevertheless, due to its complicated cycle and poor performance, vapor compression cycles are more attractive in this case.

Integrating the conventional absorption system to ejector is one of the impressive solutions. The suitable system building is able to enhance the cycle COP nearly as a multi-effect absorption chiller.

Nevertheless, because of the simple construction of the ejector/absorption cooling chiller, its initial price is relatively cheaper than other traditional efficient absorption chillers [11]. Lately, Sozen et al. suggested a solar-powered ejector- absorption cycle (shown in Fig. 14) utilizes ammonia-water refrigerant with Turkish ambient parameters.

Figure 14 –Ejector-Solar Absorption Combined Refrigeration Cycle [7].

The ejector was positioned at the inlet of the absorber that recovered the pressure from evaporator with ease. Regarding results out of this study, with the ejector usage, there was about 20% of COP increase [7].

Wang et al. analyzed a combination of ejector/absorption cooling cycle and power using ammonia-water as a working fluid. This system in Figure.15 composed of the ejector-absorption cooling cycle with Rankine cycle and can make a cooling effect and power output at the same time.

This consolidated cycle presents an ejector between the condenser and the rectifier and gives a positive change in performance without extraordinary complications in the cycle.
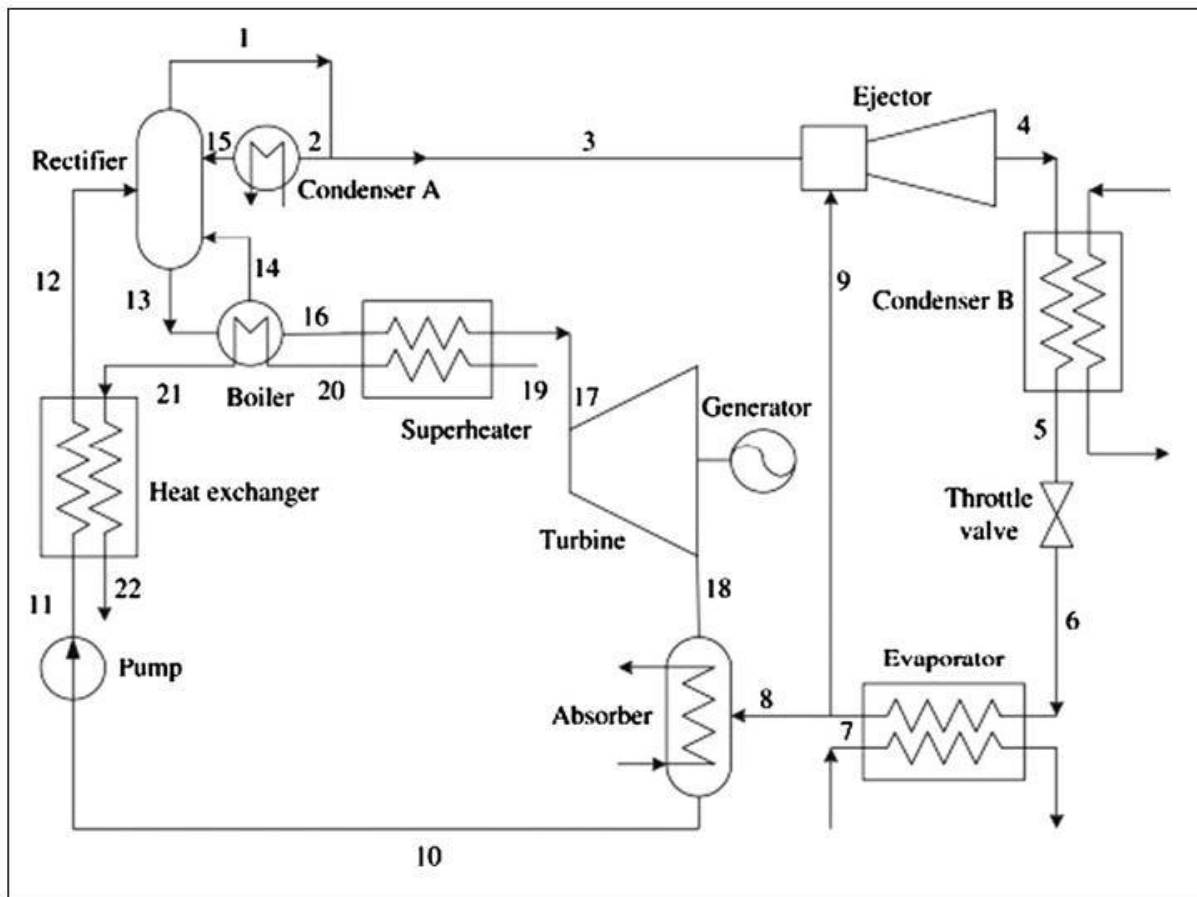
Figure 15 – Ejector-Absorption Refrigeration combined with Power Cycle [7].

The correlations of the parametric outcomes among a comparative joined cycle without ejector and this cycle demonstrated that cooling capacity raised from 149 kW to 250 kW at -8°C evaporator and generator temperature of 87°C [7].

Keeping in mind the end goal to influence adequate utilization of high-quality heat with a basic structure cooling cycle, Hong et al. suggested a novel ejector-absorption cooling cycle (appeared in Fig. 16).

At the point when the temperature of the high-temperature reservoir is sufficiently high, the system would function as a dual cycle. Both of the generators were utilized as a part of the cycle, with the goal that the pressure of the high-pressure generator and that of the low-pressure generator could be enhanced to get the highest performance for any required operating parameters.
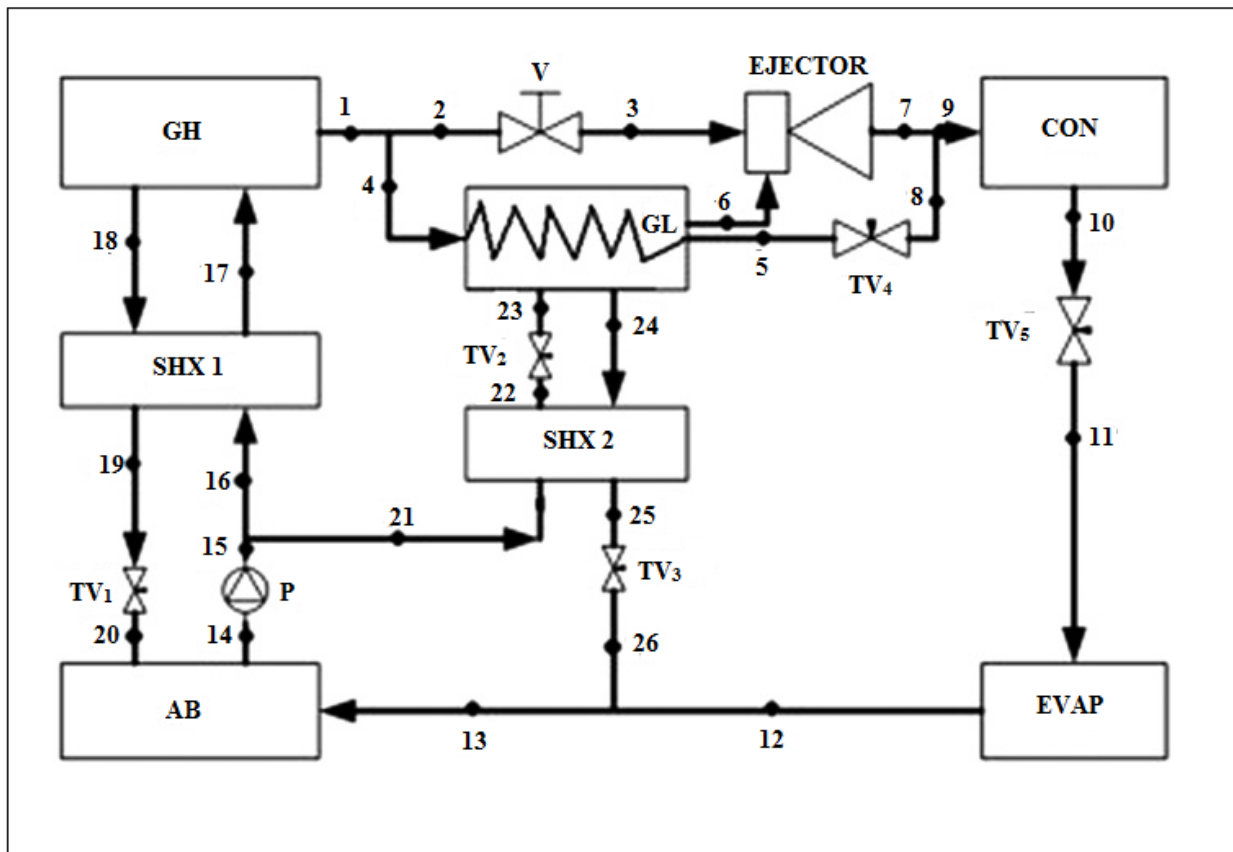
Figure 16 – Ejector-Absorption Cycle [7].

The investigation outcomes demonstrated that cycle COP was 30% greater than that of the regular absorption cooling system [7].

Notwithstanding, no testing results were accessible. Conceptual and test investigation of solar based ejector absorption cycle was investigated by Abdulateef et al [7].

The impacts of the working parameters on the COP and the refrigeration limit were examined. A numerical model was produced for outline and performance assessment of the ejector cooling systems.

1.5.   Summary of improvement methods

Ejector cooling systems excluding the usage of a pump are very attractive because of the potential for energy consumption reduction.

The suggested systems are attractive, however with low performances and the large-scale work and modeling techniques suffer from a lack of experimental

investigation. Especially the gravitational and the ejector cooling system with thermal pumping effect was studied experimentally.

Solar ejector cooling system natural convection based have a cost payback time of 33 years and current criticality, especially the huge thermal inertia, that impacts the starting and shutting down characteristics.

Furthermore, the usage of an extra burner is needed through off-design working for more heating and to avoid thermal transient. Between the various configurations, the rotational or gravitational cycle is attractive and it's potential to be used in many commercial applications (i.e. food storage, air-conditioning, etc.).

Though it's some disadvantages to be noticed, as the problematic studies while performing experiments.

Nevertheless, it must be noticed that the rotational system requires a motorized rotor powered by electric energy. Hence, this configuration works without the pump, though requires electric power.

The heat pipe-ejector system seems to be promising: the performance is expected to be close to the absorption ejector system, however in heat pipe-ejector system cost less, also doesn't need a lot of maintenance, smaller and without moving components. Lamentably, there is no available experimental analysis [7].

1.6.   Thermodynamic design and layout of the cycle

One of the targets of this study is to create a simple design of ejector cooling cycle, so this cycle will include a pump and ejector and will exclude the compressor as in figure 17 & 18 to decrease the dependence on the high-grade energy, also to decrease the maintenance and running costs. This cycle has to be designed to be used for already working systems. Environmentally friendly and safer operation. As efficient as possible.

Figure 17-Ejector cooling cycle

In figure 17 the working fluid will go through the evaporator and then through the ejector together with the fluid that comes from the generator, will mix and go to reject heat through the condenser and then split again.

Figure 18-Ejector cooling P-h diagram

The first part in figure 18 (high-pressure) will go to complete the generator cycle by increasing the pressure using a pump (4-5) and then getting the heat from the generator (5-6) and go the ejector again (6-3).

The second part (low-pressure) of the fluid will go through the expansion valve (4-1) and then to the evaporator to carry the heat from the conditioned space (1-2) and then to the ejector (2-3) and so on.

1.6.1. **Working fluid and temperatures ranges selection**

In literature, there are a lot of refrigerants that can be used in this cycle i.e. 134a, 1234yf, Ammonia, R744, R717, R123, R113, R141b, R142b, water, etc.

Considering environmental impact, availability and technical characteristics, water was found to be very suitable for this environmentally friendly project.

Also, water has very high critical pressure compared to other refrigerants (220.64 bar), which will allow using high pressures in the cycle avoiding any complexity from dealing with trans-critical cycles.

Regarding the temperature ranges, for the generator temperature depends on the automotive exhaust temperature which varies within the range of 300-600 °C.[12] For the condenser, the higher the more suitable to different weather conditions, from a practical point of view the average is about 40°C.

But for the evaporator, the lower it gets, the lower COP we obtain, also the temperature difference needs to be significant to have good heat transfer, so to achieve reasonable results the evaporator range can be from 5-10 °C.

2. Models

2.1. A mathematical model of the ejector

Motive flow in the nozzle and suction chamber

Figure 19 shows the critical sections through the ejector which is needed for calculations.
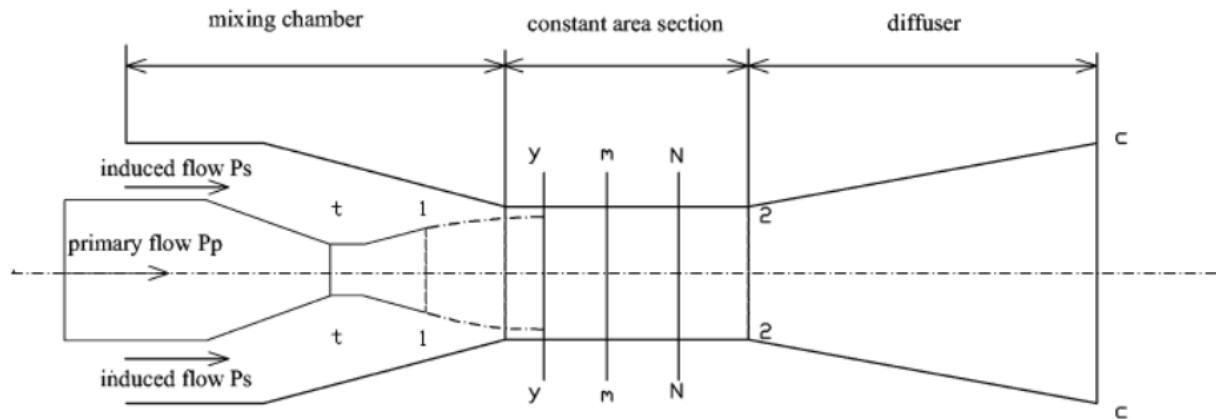
Figure 19 – Geometry and sections in ejector [3].

Considering intake total pressure, P_P, and temperature, T_P, the mass flow rate of primary flow down the nozzle, m_P, is obtained by the isentropic flow equation [3]

$$m_P = \frac{P_P A_t}{\sqrt{T_P}} \times \sqrt{\frac{\gamma}{R}\left(\frac{2}{\gamma+1}\right)^{(\gamma+1)/(\gamma-1)}} \times \sqrt{\eta_P} \qquad [1]$$

Where η_P is the isentropic efficiency of the nozzle. Utilizing conservation of energy-mass, the fluid mechanic's equations for isentropic flow between the Mach number at the nozzle exit, Mp1, the exit cross-sectional area, Ap1, and the pressure at the exit, Pp1, is obtained by

$$\left(\frac{A_{P1}}{A_t}\right)^2 = \frac{1}{M_{P1}^2}\left[\frac{2}{\gamma+1}\left(1+\frac{\gamma-1}{2}M_{P1}^2\right)\right]^{(\gamma+1)/(\gamma-1)} \qquad [2]$$

$$\frac{P_P}{P_{P1}} = \left(1+\frac{\gamma-1}{2}M_{P1}^2\right)^{\gamma/(\gamma-1)} \qquad [3]$$

Because the motive flow jets out without being mixed with the secondary flow, the primary flow from sections 1-1 to y-y is simplified utilizing isentropic

equations, and the Mach number, M_{Py}, of the motive flow at the y-y section is given by

$$\frac{P_{Py}}{P_{P1}} = \frac{\left(1+\frac{\gamma-1}{2}M_{P1}^2\right)^{\gamma/(\gamma-1)}}{\left(1+\frac{\gamma-1}{2}M_{Py}^2\right)^{\gamma/(\gamma-1)}} \qquad\qquad [4]$$

Also the cross-section area of the motive flow at the y-y section, A_{py}, can be obtained by:

$$\frac{A_{Py}}{A_{P1}} = \frac{\left(\eta_{Py}/M_{Py}\right)\left[(2/(\gamma+1))\left(1+((\gamma-1)/2)M_{Py}^2\right)\right]^{(\gamma+1)/(2(\gamma-1))}}{(1/M_{P1})\left[(2/(\gamma+1))\left(1+((\gamma-1)/2)M_{P1}^2\right)\right]^{(\gamma+1)/(2(\gamma-1))}} \qquad [5]$$

The isentropic efficiency, η_p, is considered for the primary flow losses from sections 1-1 to y-y

$$\frac{T_P}{T_{Py}} = 1 + \frac{\gamma-1}{2}M_{Py}^2 \qquad\qquad [6]$$

Induced flow from the inlet to section y-y (mixing process begins just after this section)

Critical point [3]

Regarding the operation of the critical point, it is considered that the secondary flow is chocking at section y-y. For this case, these equations can be used:

$$M_{sy} = 1, \qquad\qquad [7]$$

$$P_{sy} = P_{sy}^*, \qquad\qquad [8]$$

Also for the total pressure P_s, P^*_{sy} is calculated by

$$P_{sy}^* = P_s\left(1 + \frac{\gamma-1}{2}M_{sy}^2\right)^{-\gamma/(\gamma-1)} \qquad\qquad [9]$$

Regarding the total pressure, P_s, and temperature, T_s, h_s is the isentropic efficiency for the secondary flow, the mass flow rate of secondary flow through the nozzle, m_s, is given at critical point working condition:

$$m_s = \frac{P_s A_{sy}}{\sqrt{T_s}} \times \sqrt{\frac{\gamma}{R}\left(\frac{2}{\gamma+1}\right)^{(\gamma+1)/(\gamma-1)}} \sqrt{\eta_s} \qquad [10]$$

Sub-critical mode [3]

For sub-critical mode operation, it is assumed that there is an effective area where the velocity of the induced flow is the highest (but lowers than the speed of sound in this case). As such, the following equations are valid:

$$M_{sy} < 1 \qquad [11]$$

$$P_{sy} > P_{sy}^* \qquad [12]$$

Utilizing conservation law of energy and mass, also isentropic equations, the following equations are given:

$$\frac{T_{sy}}{T_s} = \left(\frac{P_{sy}}{P_s}\right)^{(\gamma-1)/\gamma} \qquad [13]$$

$$P_{sy} v_{sy} = R T_{sy} \qquad [14]$$

$$V_{sy} = \sqrt{2 C_P \left(T_s - T_{sy}\right)} \qquad [15]$$

$$m_s = \frac{V_{sy} A_{sy}}{v_{sy}} \sqrt{\eta_s} \qquad [16]$$

Where η_s is the isentropic efficiency coefficient of the induced nozzle. The area of section y-y is A_2 where

$$A_{py} + A_{sy} = A_2 \qquad [17]$$

A_{py} and A_{sy} are the areas for motive and secondary flow, accordingly [3].

Mixed flow at the m-m section (fluids are mixed), shock upstream [3]

Motive and secondary fluids start to form a mixture after section y-y. Utilizing the energy-momentum conservation between sections y-y and m-m, the relations include

$$\psi_m \left(m_p V_{Py} + m_s V_{sy}\right) = (m_P + m_s) V_m \qquad [18]$$

$$m_P \left(C_P T_{Py} + \frac{V_{Py}^2}{2} \right) + m_s \left(C_P T_{sy} + \frac{V_{sy}^2}{2} \right) = (m_P + m_s) \left(C_P T_m + \frac{V_m^2}{2} \right) \qquad [19]$$

Where V_m is the velocity of the mixture and ψ_m is the coefficient representing for the frictional losses (Aphornratana and Eames; Huang et al.). V_{Py} and V_{sy} are the gas velocities of motive and secondary flows at section y-y and can be calculated as

$$V_{Py} = M_{Py} a_{Py} \qquad [20]$$

$$a_{Py} = \sqrt{\gamma R T_{Py}} \qquad [21]$$

The Mach number of the mixture can be calculated utilizing these equations:

$$M_m = \frac{V_m}{a_m} \qquad [22]$$

$$a_m = \sqrt{\gamma R T_m} \qquad [23]$$

Mixed flow through the shock from m-m to 2-2 [3]

A normal shock is set to exist at section N-N. Assuming that the mixed flow after the shock undergoes an isentropic process, the mixed flow between sections m-m and 2-2 inside the constant area section has a uniform pressure, P2. Therefore, the gas dynamic relations are

$$\frac{P_2}{P_m} = 1 + \frac{2\gamma}{\gamma+1} (M_m^2 - 1) \qquad [24]$$

$$M_2^2 = \frac{1 + \frac{\gamma-1}{2} M_m^2}{\gamma M_m^2 - \frac{\gamma-1}{2}} \qquad [25]$$

The Mixture through the diffuser

The pressure recovery process of the mixed flow is obtained through going in the subsonic diffuser, considering isentropic process:

$$\frac{P_c}{P_2} = \left(1 + \frac{\gamma-1}{2} M_2^2 \right)^{\gamma/(\gamma-1)} \qquad [26]$$

Procedure

For a given nozzle throat diameter d_t (or area of nozzle throat A_t) in figure 19, nozzle exit diameter d_1 (or area of nozzle exit A_1), and constant area section diameter d_2 (or area of constant area section A_2), the performance of an ejector is characterized by the total pressure and temperature at the primary nozzle inlet (P_p, T_p), and the total pressure and temperature (P_s, T_s) at the suction chamber inlet [3].

A critical step is to calculate the value of $P*_c$, then gives a back pressure value P_c. If P_c is lower than $P*_c$, the ejector is at critical operation. Otherwise, the ejector is at sub-critical operation.

The output of the analysis includes the primary mass flow rate m_p, the secondary mass flow rate m_s and the entrainment ratio ω. In the present model, all the default coefficients are taken from Huang et al. (1999).

The coefficients accounting for the losses in the primary flow nozzle and from the exit of the nozzle to the section y-y are taken as $\eta_p = 0.95$ and $\eta_{py} = 0.88$, respectively. The coefficient accounting for the loss in the induced flow is taken as $\eta_s = 0.85$.

The coefficient accounting for the frictional loss in the mixing section, Ψ_m, is sensitive to the area ratio, A_2/A_t, such that the empirical relation presented is used [3]:

$$\psi_m = \begin{cases} 0.8, for \ A_2/A_t > 8.3 \\ 0.82, for \ 6.9 \leq A_2/A_t \leq 8.3 \\ 0.84, for \ A_2/A_t < 6.9 \end{cases} \qquad [27]$$

As specified over, the greater part of the relations is comparable with the model suggested by Huang et al. (1999) in light of a similar 1D concept based on the mass, conversations equations of energy and momentum.

However, the itemized methodology flowchart for the critical point is dissimilar. In Huang's model, P_c* the critical back pressure is a self-standing parameter (acquired from test information), and then the resolution strategy is iterated till the theoretical value of critical back pressure equalized to the experimental P_c* by varying A_2.

Hence, the entrainment ratio is obtained using the theoretical A_2 or required A_2 (not the testing result A_2). Their aim was to get the connection between the required A_2 and critical back pressure and motive pressure [3].

According to the current mock-up, the critical back pressure Pc* isn't used as an independent variable, the entrainment ratio is obtained by experimental A2 value, and Pc* is an outcome parameter.

The major goal of this study is to expect the performance of ejector for the whole operating domain for same ejector design [3].

2.2. Thermodynamic cycle model

$$\text{Cooling load} = m_s \times (h_2 - h_1) \tag{28}$$

$$\text{Gen. Power} = m_p \times (h_6 - h_5) \tag{29}$$

$$\text{Cond. load} = m_m \times (h_3 - h_4) \tag{30}$$

$$Pump\ power\ = Q \times p \times 100/\eta_{pump} \tag{31}$$

$$\text{COP} = \frac{Cooling\ load}{Pump\ power + Cond.load} \tag{32}$$

$$\text{COP}_{theoritical} = \frac{T_e}{T_g - T_e} \tag{33}$$

2.3. Heat exchanger model

The overall heat transfer coefficient calculations considering fouling resistance is given by [13]:

$$\frac{1}{\text{UA}} = \frac{1}{(\eta hA)i} + R_{f,i} + \frac{1}{Skw} + R_{f,o} + \frac{1}{(\eta hA)o} \tag{34}$$

$$P = m \cdot C_p \cdot \delta t \text{ (for sensible heat transfer)} \tag{35}$$

$$P = m \cdot \Delta h \text{ (for phase change)} \tag{36}$$

$$\text{LMTD} = \frac{\Delta T1 - \Delta T2}{\ln\frac{\Delta T1}{\Delta T2}} \tag{37}$$

$$\Delta T1 = T1 - T4 \tag{38}$$

$$\Delta T2 = T2 - T3 \tag{39}$$

3. Results

3.1. Ejector mathematical model results

In this section, the performance behavior depending on different parameters is defined.

The Effect of changing Primary, secondary pressures and temperatures on the performance curves will be elaborated in the following data.

Changing Tp total for 3 different values of Pp.

Table 3 Changing primary flow total temp. For 3 different primary pressures

	Tp K	375	390	405	420	435	450	465	480	495	510	525
Pp = 60 bar	Pc bar	0.1355	0.1357	0.1358	0.1359	0.1359	0.1359	0.1359	0.1359	0.1358	0.1357	0.1356
	ω	2.57	2.65	2.74	2.82	2.90	2.97	3.05	3.12	3.19	3.26	3.33
Pp = 80 bar	Pc bar	0.1566	0.1568	0.1569	0.1570	0.1571	0.1571	0.1572	0.1572	0.1572	0.1572	0.1572
	ω	1.94	1.98	2.02	2.05	2.09	2.12	2.16	2.19	2.23	2.26	2.29
Pp = 100 bar	Pc bar	0.1775	0.1777	0.1779	0.1780	0.1781	0.1782	0.1782	0.1783	0.1783	0.1783	0.1782
	ω	1.55	1.58	1.61	1.64	1.67	1.70	1.73	1.76	1.78	1.81	1.84
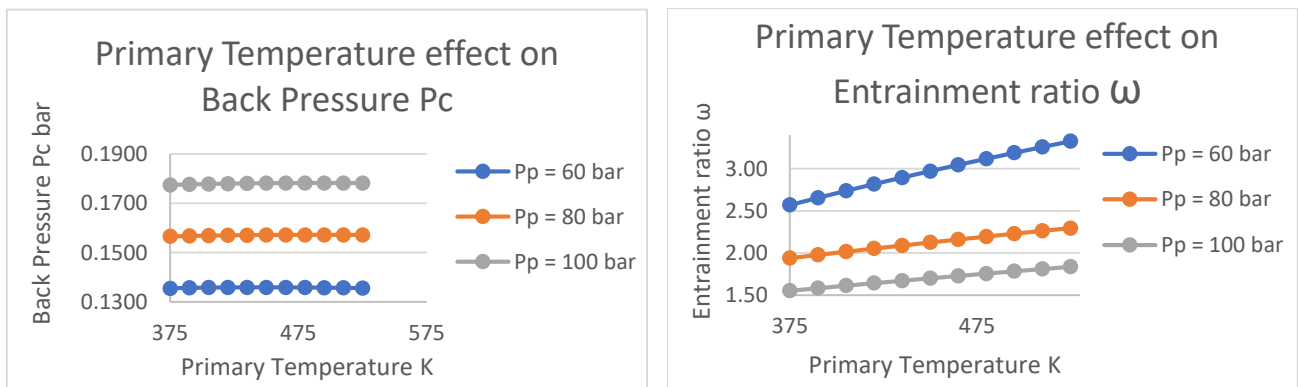
Figure 20-Back pressure and Entrainment ratio changing with primary temp.

As shown in figure 20, the back pressure didn't have that significant change driven by the primary temperature change, while the entrainment ratio noticeably increased relatively with the primary temperature increase.

In figure 21 when primary flow total pressure increases; the whole curve will be moved up showing an increase in the back pressure "p_c", also the entrainment will decrease because of the increase in the motive flow mass flow rate.
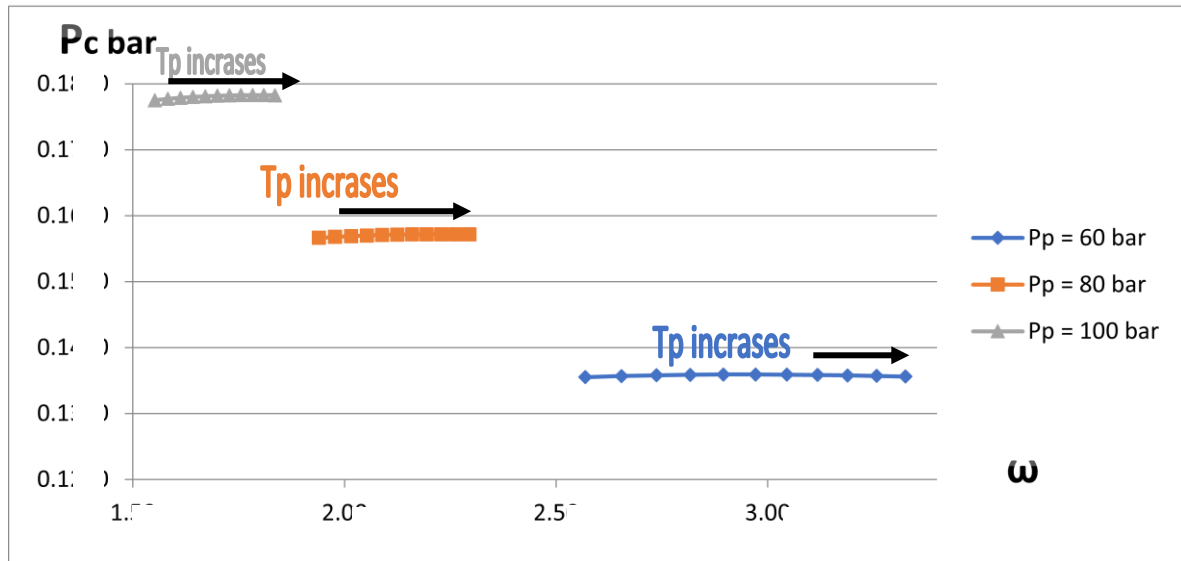
Figure 21-Back pressure change with Entrainment ratio for 3 different primary pressure values and changing primary temp.

Changing Ps for 3 different Pp values

Table 4 Changing Ps for 3 different Pp values.

	Ps bar	0.4	0.6	0.8	1	1.2	1.4	1.6	1.8	2	2.2	2.4
Pp = 60 bar	Pc bar	0.37	0.53	0.69	0.85	1.01	1.17	1.34	1.5	1.66	1.8	1.99
	ω		12.8	19.2	25.6	32	38.4	44.8	51.2	57.5	63.9	70.3	76.7
Pp = 80 bar	Pc bar	0.382	0.540	0.7	0.861	1.022	1.184	1.346	1.509	1.67	1.83	2
	ω		9.59	14.39	19.18	23.98	28.77	33.57	38.36	43.16	48	52.8	57.5
Pp = 100 bar	Pc bar	0.401	0.556	0.715	0.875	1.036	1.197	1.359	1.521	1.67	1.85	2.01
	ω		7.67	11.51	15.34	19.18	23.02	26.85	30.69	34.52	38.36	42.2	46
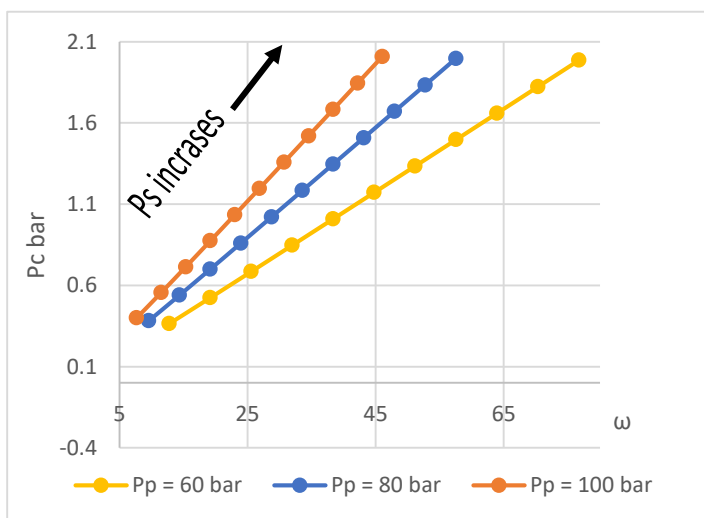
(a)
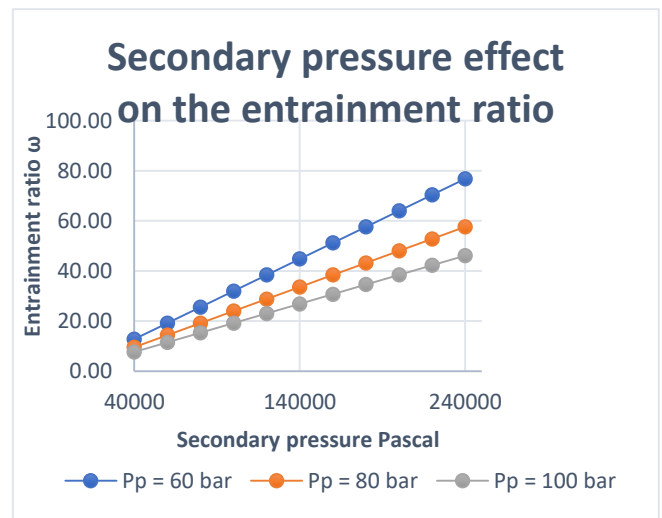
(b)

Figure 22- Back pressure change with Entrainment ratio for 3 different primary pressure values and changing sec. pressure.

27

When P_p increases in P_c increases, also ω decreases because of the increase of the motive flow rate in figure 22 (a). As the secondary pressure raises, the entrainment ratio increases too figure 22 (b).

Changing Pp for 3 different values of Ps

Table 5 Changing Pp for 3 different values of Ps.

	Pp bar	5	10	15	20	25	35	45	55	65	75	85
Ps= 0.1 bar	Pc bar	0.084	0.088	0.09	0.096	0.1	0.11	0.12	0.13	0.14	0.152	0.162
	ω		38.36	19.18	12.8	9.59	7.67	5.48	4.26	3.49	2.95	2.56	2.26
Ps= 0.2 bar	Pc bar	0.166	0.168	0.17	0.175	0.18	0.19	0.196	0.21	0.22	0.225	0.235
	ω	76.72	38.36	25.6	19.18	15.34	11	8.52	6.97	5.90	5.11	4.51
Ps= 0.3 bar	Pc bar	0.247	0.25	0.25	0.256	0.26	0.27	0.274	0.28	0.29	0.3	0.31
	ω	105.5	52.74	35.2	26.37	21.1	15.1	11.72	9.59	8.11	7.03	6.20

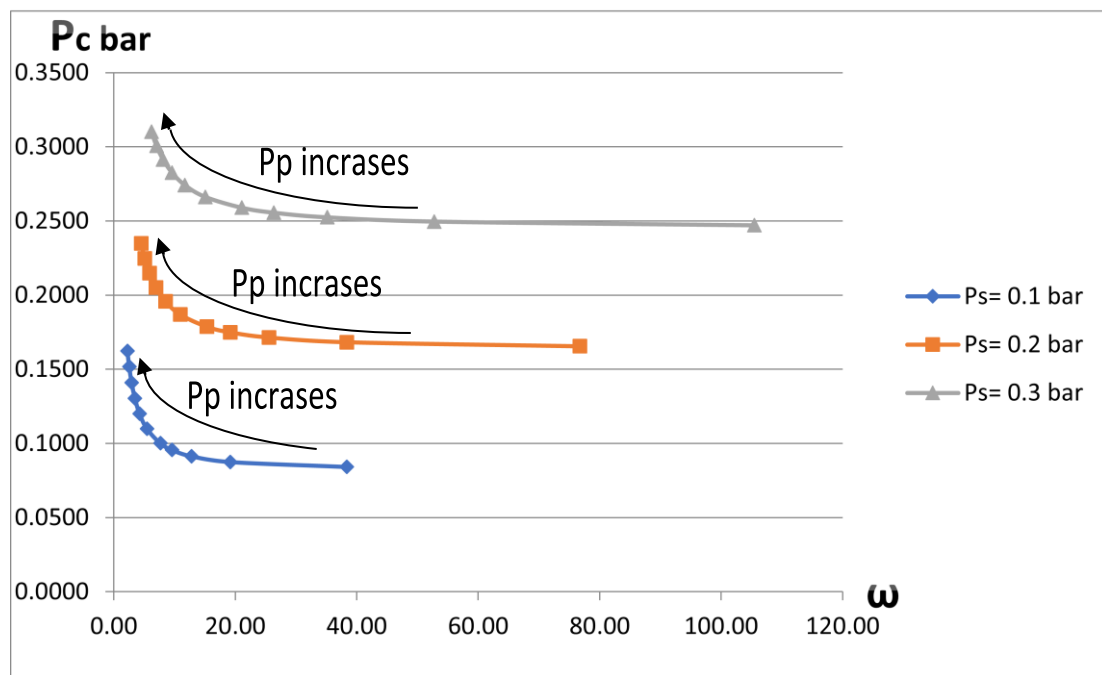Figure 23- Back pressure change with Entrainment ratio for 3 different secondary pressure values and changing primary pressure.

When P_p increases in figure 23, P_{sy} and P_{py} increase which increases P_2 and therefore P_c increases and ω increases because of boosting the induced flow rate.

Also when the secondary pressure rises, the entrainment ratio steps up. Due to the secondary flow rate increase.

Sub-Critical mode iterations

Table 6 Sub-Critical mode iterations

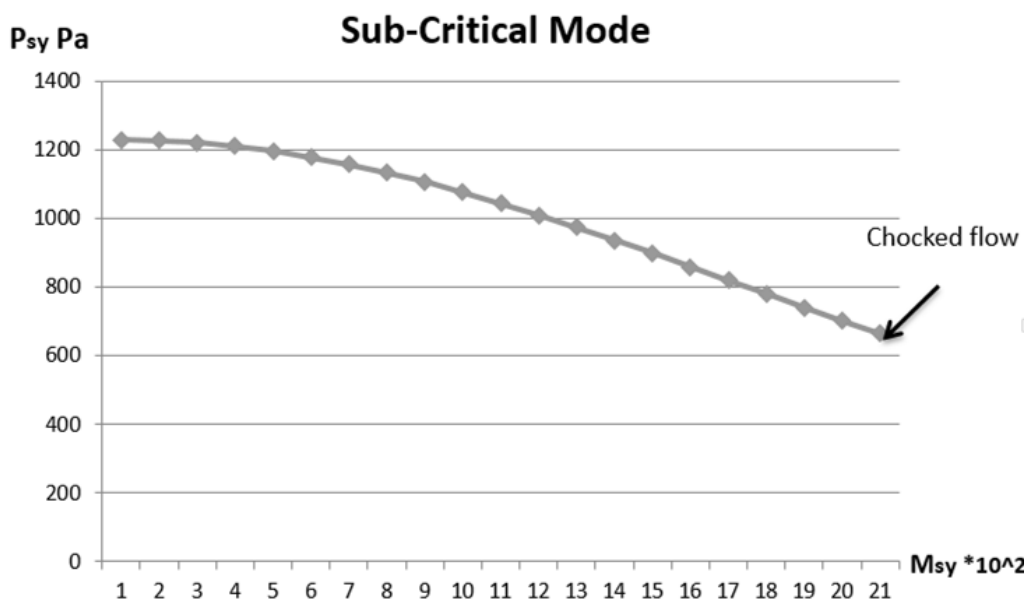| Sub-Critical Mode					
Msy	Psy Pa	Tsy K	Vsy m/s	v m3/kg	ms kg/s
0	1228	286.00	0.00	198.91	0.0000
0.05	1225.961	285.88	31.40	198.83	0.0004
0.1	1219.868	285.53	62.76	198.58	0.0007
0.15	1209.796	284.94	94.04	198.17	0.0011
0.2	1195.87	284.12	125.21	197.60	0.0015
0.25	1178.258	283.08	156.22	196.88	0.0019
0.3	1157.169	281.82	187.05	196.00	0.0022
0.35	1132.85	280.33	217.65	194.97	0.0026
0.4	1105.577	278.64	247.99	193.79	0.0030
0.45	1075.65	276.75	278.04	192.48	0.0034
0.5	1043.389	274.67	307.77	191.03	0.0038
0.55	1009.125	272.40	337.14	189.45	0.0042
0.6	973.1933	269.96	366.14	187.76	0.0046
0.65	935.9296	267.36	394.74	185.95	0.0050
0.7	897.6633	264.61	422.91	184.03	0.0054
0.75	858.7123	261.71	450.63	182.02	0.0058
0.8	819.3795	258.68	477.88	179.91	0.0062
0.85	779.9486	255.54	504.65	177.72	0.0066
0.9	740.6815	252.28	530.92	175.46	0.0071
0.95	701.8167	248.93	556.68	173.13	0.0075
1	663.567	245.49	581.92	170.74	0.0080

Figure 24-Sec. pressure change with Mach no. in the sub-critical mode.

It describes the effect of the Mach no. at the start of the mixing section (Y-Y) Fig. 19 on the secondary pressure at the same point. When the Mach no. increases the pressure decreases, which is logical according to the isentropic equations for ideal gases.

3.2.   Ejector mathematical model iterations

From all iterations that were done, some of them were chosen to clarify the effect of changing the throttle diameter on the COP and the condenser temperature, to figure out the most suitable configuration for our requirements.

Dt = 0.001 m, generator temp. = 300 C, Primary pressure = 80 bar

Table 7(a) Dt = 0.001 m, generator temp. = 300 C, Primary pressure = 80 bar iteration

Flow Sec.	Primary flow			Secondary flow		Mixed Flow		
	throttle	1-1	Y-Y	1-1	Y-Y	m-m	2-2	C-C
D (m)	0.001				0.045		0.047983	
A (m2)	7.854E-07	1.3707E-06	0.000218		0.00159		0.001808	
M	1	2	7.51		1	2.54	0.495	
m (Kg/s)	0.0082	0.0082	0.0082	0.0036	0.0036	0.0118	0.0118	
P (Pa)	8000000	1037499.01	663.57		663.57		4801.96	5633.93
T (K)	573	345.18	55.66		245.49	189.26		
V (m/s)			1387.26		388.18	866.46		
η	0.99	0.99	0.95	0.98	0.98			

Table 7(b) Dt = 0.001 m, generator temp. = 300 C, Primary pressure = 80 bar iteration

Rg (KJ/Kg K)	461.5	Pump Power (KW)	0.0654
γ	1.33	Cooling load (KW)	8.528
Ψm	0.80	Gen. Power (KW)	21.62
ω	0.44	Cond. load (KW)	30.476
Cond. Temp. (K)	308	COP	0.3933
Cp (J/Kg K)	4180.00	COP theoretical	0.9757

In this iteration as shown the throttle diameter is only 1 mm, condenser temperature is 35 C, and the COP is 0.393, which is really good for an ejector cooling cycle.

Dt = 0.0012 m, generator temp. = 300 C, Primary pressure = 80 bar

Table 8 (a) 2.8.2.   Dt = 0.0012 m, generator temp. = 300 C, Primary pressure = 80 bar iteration

Flow Sec.	Primary flow			Secondary flow		Mixed Flow		
	throttle	1-1	Y-Y	1-1	Y-Y	m-m	2-2	C-C
D (m)	0.0012				0.045		0.049239	
A (m2)	1.131E-06	1.9739E-06	0.000314		0.00159		0.001904	
M	1	2	7.51		1	2.79	0.474	
m (Kg/s)	0.0118	0.0118	0.0118	0.0036	0.0036	0.0154	0.0154	
P (Pa)	8000000	1037499.01	663.57		663.57		5798.05	6712.64
T (K)	573	345.18	55.66		245.49	178.64		
V (m/s)			1387.26		388.18	923.48		
η	0.99	0.99	0.95	0.98	0.98			

Table 8 (b) Dt = 0.0012 m, generator temp. = 300 C, Primary pressure = 80 bar iteration

R_g (KJ/Kg K)	461.5	Pump Power (KW)	0.094
γ	1.33	Cooling load (KW)	8.4833
Ψ_m	0.80	Gen. Power (KW)	30.9853
ω	0.30	Cond. load (KW)	39.4091
Cond. Temp (K)	311.2	COP	0.273
C_p (J/Kg K)	4180.00	COP theoretical	0.9759

It's very clear that when the throttle diameter increased keeping the other given parameters, the condenser pressure increased and so does the condenser temperature to be 38.2 C.

On the other hand, the COP decreased as the generator load increased for the same cooling load.

Dt = 0.0014 m, generator temp. = 300 C, Primary pressure = 80 bar

Table 9(a) Dt = 0.0014 m, generator temp. = 300 C, Primary pressure = 80 bar

Flow Sec.	Primary flow			Secondary flow		Mixed Flow		
	throttle	1-1	Y-Y	1-1	Y-Y	m-m	2-2	C-C
D (m)	0.0014				0.045		0.050682	
A (m2)	1.5394E-06	2.6867E-06	0.000427		0.00159		0.002017	
M	1	2	7.51		1	2.98	0.460	
m (Kg/s)	0.0160	0.0160	0.0160	0.0036	0.0036	0.0196	0.0196	
P (Pa)	8000000	1037499.01	663.57		663.57		6625.64	7609.37
T (K)	573	345.18	55.66		245.49	170.65		
V (m/s)			1387.26		388.18	963.89		
η	0.99	0.99	0.95	0.98	0.98			

Table 9(a) Dt = 0.0014 m, generator temp. = 300 C, Primary pressure = 80 bar

Rg (KJ/Kg K)	461.5	Pump Power (KW)	0.1281
γ	1.33	Cooling load (KW)	8.4546
Ψm	0.80	Gen. Power (KW)	42.0462
ω	0.22	Cond. load (KW)	50.7431
Cond. Temp (K)	313.56	COP	0.2005
Cp (J/Kg K)	4180.00	COP theoretical	0.9759

The COP is decreased as expected; on the other hand, the temperature of condenser has increased to be 40.56 C which is more favorable.

Dt = 0.0016 m, generator temp. = 300 C, Primary pressure = 80 bar

Table 10(a) Dt = 0.0016 m, generator temp. = 300 C, Primary pressure = 80 bar

	Primary flow			Secondary flow		Mixed Flow		
Flow Sec.	throttle	1-1	Y-Y	1-1	Y-Y	m-m	2-2	C-C
D (m)	0.0016				0.045		0.052298	
A (m2)	2.0106E-06	3.5091E-06	0.000558		0.00159		0.002148	
M	1	2	7.51		1	3.12	0.451	
m (Kg/s)	0.0209	0.0209	0.0209	0.0036	0.0036	0.0245	0.0245	
P (Pa)	8000000	1037499.01	663.57		663.57		7299.86	8340.13
T (K)	573	345.18	55.66		245.49	164.63		
V (m/s)			1387.26		388.18	993.10		
η	0.99	0.99	0.95	0.98	0.98			

Table 10(b) Dt = 0.0016 m, generator temp. = 300 C, Primary pressure = 80 bar

Rg (KJ/Kg K)	461.5	Pump Power (KW)	0.1673
γ	1.33	Cooling load (KW)	8.4235
Ψm	0.80	Gen. Power (KW)	54.7354
ω	0.17	Cond. load (KW)	63.676
Cond. Temp (K)	315.3	COP	0.1534
Cp (J/Kg K)	4180.00	COP theoretical	0.9759

As shown, the COP decreased significantly, when the condenser temperature increased to 42 C that means it's a necessity to balance between the COP and condenser temperature.

Dt = 0.00126 m, generator temp. = 300 C, Primary pressure = 80 bar

Table 11(a) Dt = 0.00126 m, generator temp. = 300 C, Primary pressure = 80 bar

Flow Sec.	Primary flow			Secondary flow		Mixed Flow		
	throttle	1-1	Y-Y	1-1	Y-Y	m-m	2-2	C-C
D (m)	0.00126				0.045		0.04966	
A (m2)	1.25E-06	2.18E-06	0.00035		0.0016		0.00194	
M	1	2	7.51		1	2.85	0.469	
m (Kg/s)	0.013	0.013	0.013	0.0036	0.0036	0.0166	0.0166	
P (Pa)	8000000	1037499	663.57		663.57		6063.7	7000.43
T (K)	573	345.18	55.66		245.49	176		
V (m/s)			1387.26		388.18	937.06		
η	0.99	0.99	0.95	0.98	0.98			

Table 12(b) Dt = 0.00126 m, generator temp. = 300 C, Primary pressure = 80 bar

Rg (KJ/Kg K)	461.5	Pump Power (KW)	0.1038
γ	1.33	Cooling load (KW)	8.4654
Ψm	0.80	Gen. Power (KW)	34.0964
ω	0.30	Cond. load (KW)	42.6415
Cond. Temp (K)	311.2	COP	0.2475
Cp (J/Kg K)	4180.00	COP theoretical	0.9759

This iteration has an acceptable value COP, besides 38 C as a condenser temperature, which is practically suitable for normal operating conditions.

Dt = 0.00152 m, Ds = 0.065 m, generator temp. = 330 C, Primary pressure = 110 bar

Table 13(a) Dt = 0.00152 m, Ds = 0.065 m, generator temp. = 330 C, Primary pressure = 110 bar

Flow Sec.	Primary flow			Secondary flow		Mixed Flow		
	throttle	1-1	Y-Y	1-1	Y-Y	m-m	2-2	C-C
D (m)	0.00152				0.065		0.070964	
A (m2)	1.815E-06	3.167E-06	0.000637		0.00332		0.003955	
M	1	2	7.84		1	2.86	0.469	
m (Kg/s)	0.0253	0.0253	0.0253	0.0075	0.0075	0.0328	0.0328	
P (Pa)	11000000	1426561.2	663.57		663.57		6082.67	7021
T (K)	603	363.25	54.12		245.49	181.67		
V (m/s)			1428.92		388.18	953.51		
η	0.99	0.99	0.95	0.98	0.98			

Table 13(b) Dt = 0.00152 m, Ds = 0.065 m, generator temp. = 330 C, Primary pressure = 110 bar

Rg (KJ/Kg K)	461.5	Pump Power (KW)	0.2784
γ	1.33	Cooling load (KW)	17.6683
Ψm	0.80	Gen. Power (KW)	66.5283
ω	0.29	Cond. load (KW)	84.3009
Cond. Temp (K)	312.1	COP	0.2645
Cp (J/Kg K)	4180.00	COP theoretical	0.8844

This iteration has higher COP than the previous cycles, because of the increase of generator temp. and pressure with 1-degree higher condenser temperature.

Dt = 0.00128 m, Ds = 0.0548 m, generator temp. = 330 C, Primary pressure = 110 bar

Table 14(a) Dt = 0.00128 m, Ds = 0.0548 m, generator temp. = 330 C, Primary pressure = 110 bar

Flow Sec.	Primary flow			Secondary flow		Mixed Flow		
	throttle	1-1	Y-Y	1-1	Y-Y	m-m	2-2	C-C
D (m)	0.00128				0.0548		0.059817	
A (m2)	1.29E-06	2.2458E-06	0.00045		0.00236		0.00281	
M	1	2	7.84		1	2.85	0.469	
m (Kg/s)	0.0180	0.0180	0.0180	0.0053	0.0053	0.0233	0.0233	
P (Pa)	11000000	1426561.1	663.57		663.57		6076.16	7013.94
T (K)	603	363.25	54.12		245.49	181.73		
V (m/s)			1428.92		388.18	953.17		
η	0.99	0.99	0.95	0.98	0.98			

Table 14(b) Dt = 0.00128 m, Ds = 0.0548 m, generator temp. = 330 C, Primary pressure = 110 bar

Rg (KJ/Kg K)	461.5	Pump Power (KW)	0.1974
γ	1.33	Cooling load (KW)	12.5582
Ψm	0.80	Gen. Power (KW)	47.178
ω	0.30	Cond. load (KW)	59.813
Cond. Temp (K)	312.1	COP	0.265
Cp (J/Kg K)	4180.00	COP theoretical	0.8844

After diameters optimizations, this cycle obtained the highest COP with a reasonable condenser temperature of 39.1 C.

So, it'll be selected and discussed further in this paper for components selections, such as the pump, heat exchangers and expansion valve.

For thermodynamics calculations for this cycle, the specific enthalpies have to be obtained.

During calculations, Zittau's Fluid Properties Calculator will be used to figure out the working fluid (water) properties through the cycle.

Table 15 Thermodynamic values of the cycle

Point	Temperature T (K)	Pressure P (Bar)	Enthalpy h (kJ/kg)
1	283	0.01228	159.2
2	286	0.01228	2524.9
3	401.52	0.0701394	2730
4	311	0.0701394	159.2
5	309.33	80	159.2
6	573	80	2786.37

4. Refrigerant pump

There are many types of pumps to use in this cycle and here some of it

4.1. Positive Displacement Pumps [14]

This sort of pump makes an expanding volume on the suction side of the pump and a contracting volume on the outlet. This distinction makes pressure which pulls and pushes a liquid all the while, applying enough force to make a stream.

Positive displacement pumps have two different categories

Reciprocating pump

Regarding this category, the vacuum is created using a piston which plunges into and pulls out of the material. Valves are utilized to make sure that it flows only in one way. That's why the reciprocating pump pumps the liquid at similar periods.
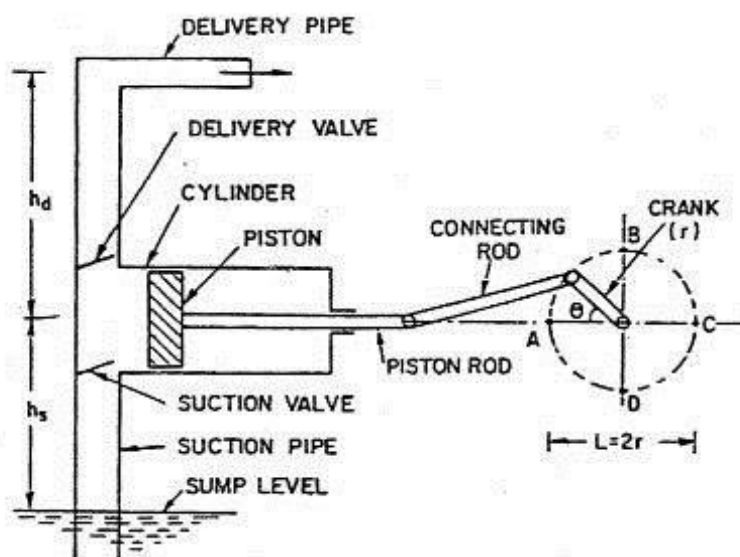

Figure 25-Plunger pump scheme [14].

Rotary (i.e. gear) pump

The rotary pump utilizes two gears that engage together. The motion of the gears generates high pressure on the outlet side which drives the flow.
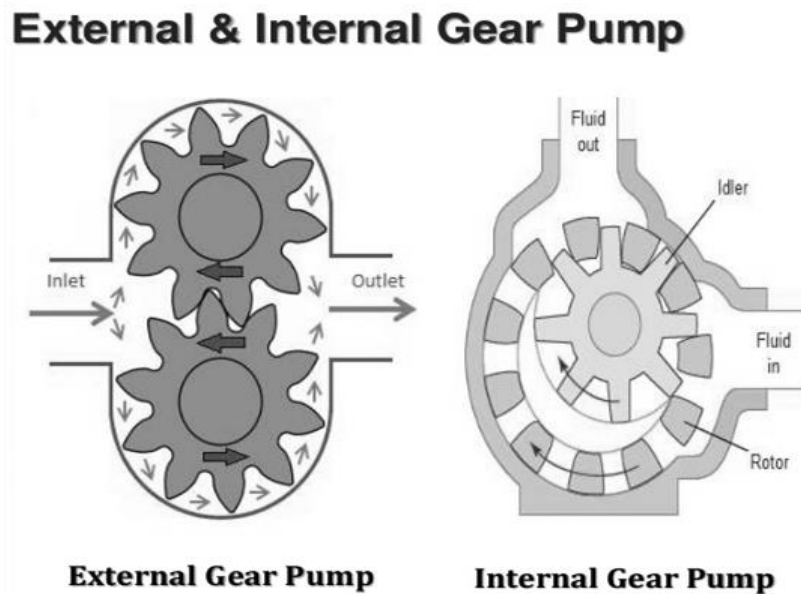

Figure 26-Gear pump [14].

Because of the design, positive displacement pumps handle viscous material better.

4.2. Centrifugal Pumps [14]

This kind of pump is one of the most common in use today. Like other pump designs, it uses an impeller, which is a rotating blade to generate suction which then moves fluid through pipes.

The rotating impeller creates what is known as centrifugal force, giving this pump design its name. The pump can be driven by an electric motor or engine. Centrifugal pumps are usually used for liquids which are low in viscosity and low in solid concentration.

However, there is a centrifugal slurry pump which can move liquids with a large number of particles.

Australian Pump Technical Handbook, The PIA (2007, p.30) categories impellers into three different designs

Axial Flow

The axial flow impeller discharges fluid along the shaft axis. For this reason, an axial flow pump is by definition not "centrifugal" in its pumping action.

Radial Flow

The fluid is discharged radially from the impeller perpendicularly to the shaft axis.

Mixed Flow

The fluid discharges from the impeller in a conical direction utilizing a combined axial and radial pumping action.
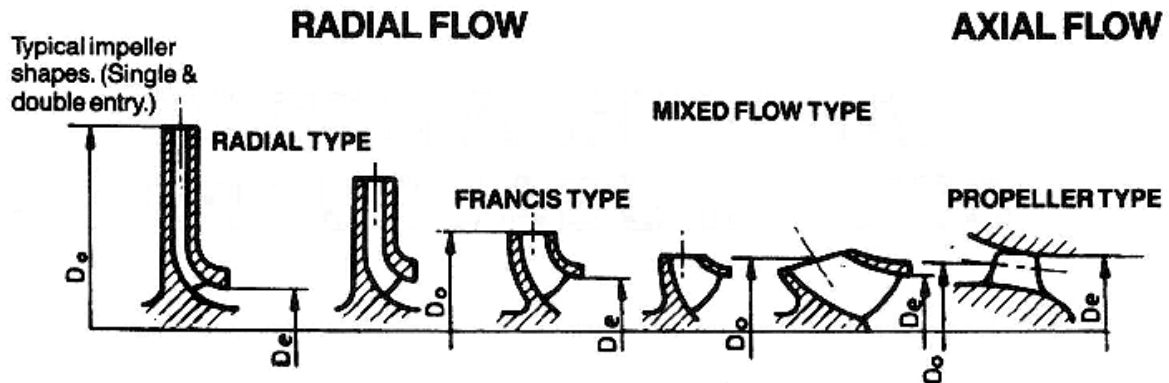

Figure. 27-Pump flow types [14].

For the ejector cooling system, it requires high pressure so; the reciprocating (Plunger) pump is more suitable in this case.

4.3.   Pump selection

From CAT Pumps co.

Model: 4DX03ELR 4DX DIRECT DRIVE PLUNGER PUMP [15]

Table 16 Plunger pump specs.

Pump specs.		Required specs.
Max Flow:	1.14 lpm	1.08 lpm
Min Pressure:	6.89 bar	
Max Pressure:	137.90 bar	110 bar
Inlet Port Size:	3/8"NPT(F)	
Discharge Port Size:	3/8"NPT(M)	
RPM:	1750	
Drive Type(s):	Direct	
Material:	Brass (BB)	

This is a triplex (3-pistons) pump that uses an electric motor, it's quite reliable for high-pressure applications when the flow rate is not high.

5. Heat exchangers

The heat exchanger is defined as a thermal equipment, which mainly designed to transfer or exchange thermal energy, from one fluid to different fluid depending on the temperature differences.

There are various types of the heat exchangers, it can be categorized according to the flow directions cross-flow, parallel-flow, or countercurrent.

For the parallel flow heat exchangers, the cold and hot fluids are moving in parallel to each other.

In cross flow exchangers, the cold and hot fluids are moving perpendicular to each other. This has the potential to produce the compact device, however, the countercurrent heat exchanger is more efficient.

In the countercurrent heat exchanger, the hot fluid enters from the right, it cools against the already warmed up cold fluid from the left. The temperature differential is nowhere near as high as at the start of the parallel heat exchanger.

However, as the temperature of the warm fluids drops, it gets exposed to the even colder cool fluid. This results in far more efficient cooling - which explains why counter flow is by far the dominant way to operate a heat exchanger.

5.1. Popular heat exchangers types

- Shell and tube heat exchanger [16]

It's combined with a number of pipes that have a fluid going through it. The pipes are split into two groups: the 1st group carries the fluid to be cooled or heated.
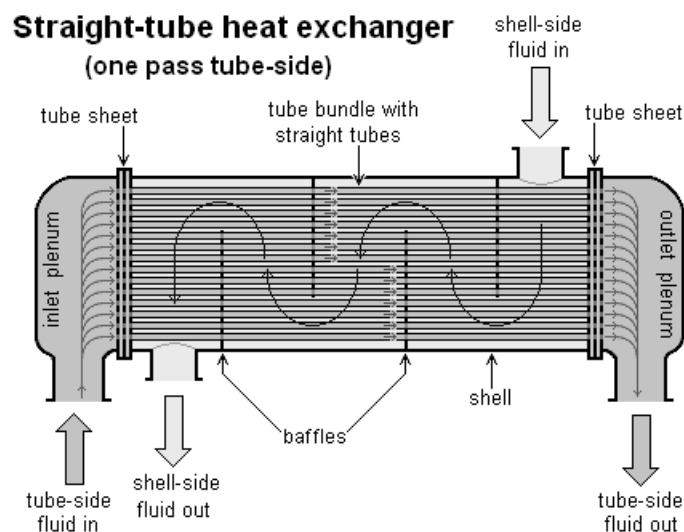

Figure 28-Strait shell and tube heat exchanger [16].

The 2nd group carries the fluid that drives the heat exchange, by adding or absorbing heat from or to the first group of pipes. While creating the design of this kind of exchanger, tube wall thickness and tube diameter must be selected carefully, to optimize heat exchanger efficiency.

- Plate heat exchangers
  Plates are made of thin material and connected together, with a narrow space between each other, usually kept by a rubber gasket.
  It's a big surface area, and the opening at corners of each rectangular plate through which fluid can pass through plates, transfer heat from the plates.

  The passages of fluid itself interchange cold and hot fluids, implying that heat exchangers can efficiently transfer heat. Thanks to having a plate with the large surface area in the heat exchangers, they are usually more effective than the shell and tube types.
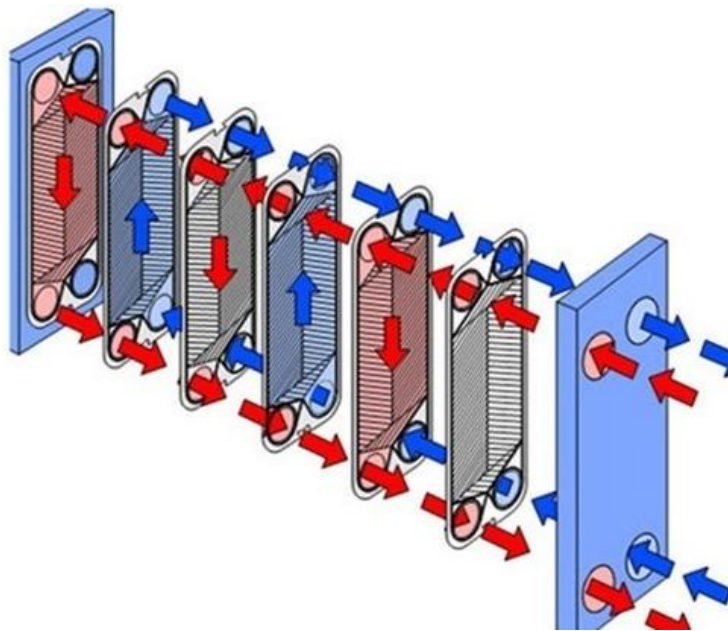

Figure 29-Plate heat exchanger [16].

- Regenerative Heat Exchanger
  For this type of heat exchangers, the same working fluid is flowing through both sides of the device, which can be either a shell and tube heat exchanger or a plate heat exchanger.

  Since the fluid temperature may increase steeply, the incoming fluid is used to cool the exiting fluid, keeping almost same temperature.

A great value of energy can be saved through a regenerative heat exchanger because the process is recurring, with roughly most of the heat being transferred from the discharging fluid to the entering fluid. For keeping the same temperature, only a little more heat requires to increase and decrease the overall fluid temperature.
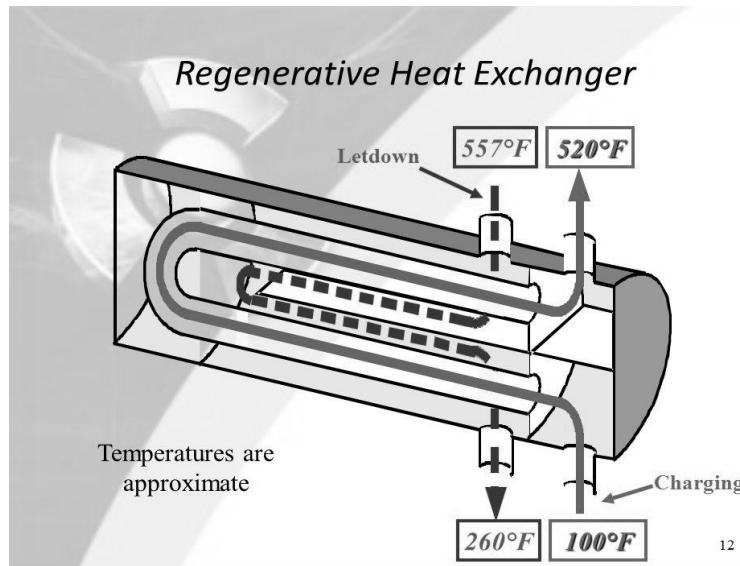

Figure 30-Regenerative heat exchanger [16].

For designing a suitable test unit for the ejector cooling system, the plate heat exchanger is more suitable for testing and experiments.

5.2.   Heat exchangers selection

Condenser selection [17]

R095 from Kaori

It's the newly-developed BPHE dedicated to environment-friendly and high thermal transferring refrigerant. Its 10% higher efficiency than conventional BPHE and lightweight significantly reduce the carbon emission.

Table 17 Condenser specs.

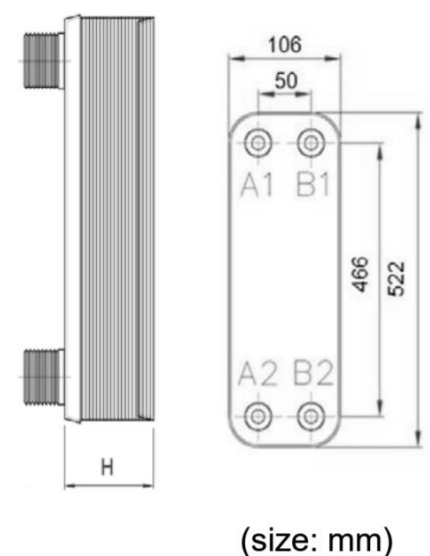|	
Max. heat load (kW)	70.32
Max. working temperature °C	200
Min. test pressure (bar)	43
Max. number of plates (N)	120
Thickness (mm) - H	10.0+1.85*N
Weight (kg)	2.73+0.154*N
Max. working pressure (bar)	30
Max. flow rate (LPM)	250
Plate Heat Transfer Area (M2)	0.0475m^2

(size: mm)

Figure 31-Kaori condenser [17].

As shown, it can handle mass flow rate up to 250 LPM, which is a lot more than what our cycle needs.

Regarding the negative pressure, it's not mentioned in the technical data, but it's possible to contact the company and ask about their negative pressure test for the design validation.

Generator selection [18]

SIGMASHELL Laser-welded plate heat exchanger for liquids, vapor, and gases from Schmidt® SIGMASHELL.

Working conditions borders: - Operating pressure from vacuum up to 150 barg. Temperature operation range from -200°C up to 550°C.

Figure 32-Schmidt® SIGMASHELL heat exchanger [18].

Evaporator selection
R050 from Kaori

 It's the same series as the condenser.

Table 18 Evaporator specs.

Max. heat load (KW)	35.16
Max. working temperature °C	200
Min. test pressure (bar)	43
Max. number of plates (N)	120
Thickness (mm) - H	10.0+1.80*N
Weight (kg)	1.32+0.089*N
Max. working pressure (bar)	30
Max. flow rate (LPM)	240
Plate Heat Transfer Area (M2)	0.0255 m^2
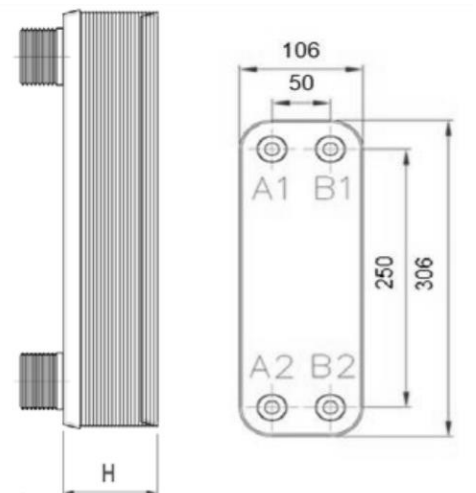
Figure 33-Kaori evaporator [17].

Still no information regarding negative pressure, but can be found from the manufacturer.

6.   Expansion Valve

Expansion valve balance equations [19]

P1+P4 = P2+P3
P1 = Bulb Pressure (Opening Force)
P2 = Evaporator Pressure (Closing Force)
P3 = Superheat Spring Pressure (Closing Force)
P4 = Liquid Pressure (Opening Force)

Expansion valve selection [20]

There are many types of expansion valves, but the most common are TXV's (thermal expansion valve) and EXV's (electronic expansion valves).

For this testing cycle, it's preferable to use the EXV as it's more flexible, adjustable, reliable and very precise control.

E2V Carel ExV

It's used for loads up to 40KW, dual directions and fits in all sizes.

Figure 34-Electronic Expansion valves EXV [20].

7. Test cycle summary

The designed testing platform components are summarized in the following table:

Table 19 Test Cycle Components

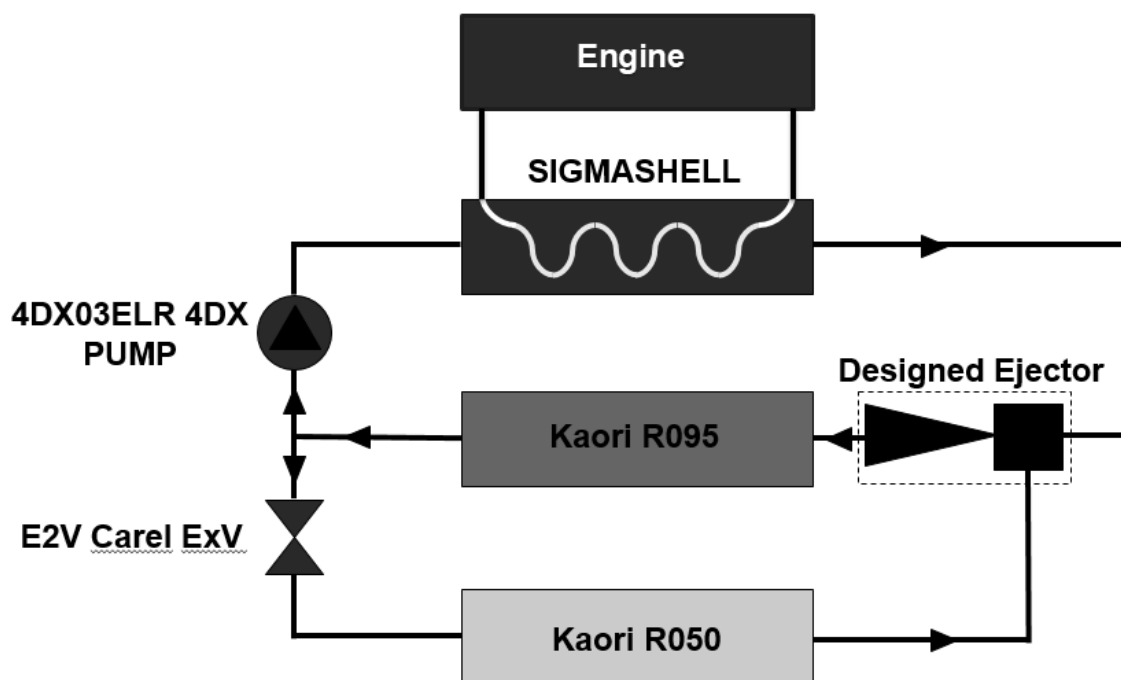| Component	Model
Generator (Heat exchanger)	SIGMASHELL Laser-welded plate heat exchanger for liquids, vapor, and gases from Schmidt® SIGMASHELL.
Condenser (Heat exchanger)	R095 from Kaori
Evaporator (Heat exchanger)	R050 from Kaori
Ejector	As Designed
Pump (reciprocating)	4DX03ELR 4DX DIRECT DRIVE PLUNGER PUMP
Expansion Valve (EXV)	E2V Carel ExV

Figure 35-cycle scheme with the selected components

As shown in figure 35, the base cycle consists mainly of three heat exchangers; the generator (SIGMASHELL), the condenser (Kaori R095) and the evaporator (Kaori R050) were selected for reliable and feasible experimenting, besides the designed Ejector and the expansion valve (E2V Carel ExV) which is an electronic expansion valve for precision and accuracy aspects.

Also the triplex plunger (reciprocating) pump (4DX03ELR 4DX), where chosen for the reliability and flexibility of operation under high pressure.

8. Conclusion

The world is wasting extraordinary amount of energy as waste heat every day through different ways that can be used relatively efficiently through the ejector-based cycles, which will save millions of tons of fossil fuel every year in hot areas i.e. (India, Mediterranean counties, Australia, South America and parts of North America, major parts of Asia, Africa, etc.).

Ejector cooling system is a promising technology for producing a cooling effect by using low-grade energy sources with different working fluids. In this paper, ejector technology, refrigerant properties and their influence over the ejector performance, the ejector refrigeration cycle was optimized for testing to dedicate results for automotive and HVAC applications.

The simplicity and reliability of ejectors, through the absence of moving parts, promote the usage of it in mass production industries, such as automotive. Especially with the desperate need to increase fuel efficiency is pushing towards the usage of waste heat.

Ejector allows the use of many refrigerants and many studies have tested the influence of the fluid on the refrigeration cycle.

Both experimental and numerical studies have shown that operating conditions critically affect the optimum performance of an ejector. Slight changes in operating conditions result in the ejector operating away from its designed optimum performance

Therefore, it is necessary to have variable geometry to cope with the variation of operating conditions, so as to give optimum performance in off-design conditions.

For most of the average vehicles with internal combustion engines have a range of 300-600 °C for exhaust gases temperatures. As a result of the mathematical model calculations and the operating conditions, in this cycle, we used 330 °C. Also the reasonable condenser temperature of 39.1 °C, and evaporator temperature of 10 °C.

Due to seeking balanced economic aspects and minimum environmental impacts, water has been assessed for our cycle which resulted in reasonable COP of 0.265 and compatible with the previously selected parameters. Whereas, the trans-critical cycles complexities have been avoided due to having the high critical pressure of water (220.64 bar).

After optimizing the cycle design, the other components were selected to complete the test-platform, such as the heat exchangers (generator, condenser, and evaporator), it was meant to be plate heat exchangers as it's more compact and suitable for experimenting besides its availability, then the pump was selected to be triplex pump (3-piston pump), as it's very much fitting with high-pressure requirements especially with the adjustable pressure possibility and finally the Expansion valve which was chosen to be EXV (electronic expansion valve), due to the flexibility and accuracy of changing the cooling loads and operating conditions.

In this paper, the versatility of ejector cooling systems which can be used in automotive applications has been demonstrated. I hope that this contribution will encourage new ideas and further research interest into the design and application of ejectors.

9. References

[1] LITTLE, Adrienne B a Srinivas GARIMELLA. A critical review linking ejector flow phenomena with component-and system-level performance. *International Journal of Refrigeration*. 2016, **70**, 243–268. ISSN 0140-7007.

[2] CHEN, Jianyong, Björn PALM a Per LUNDQVIST. Ejector Cooling System. nedatováno, 5.

[3] CHEN, Weixiong, Ming LIU, Daotong CHONG, Junjie YAN, Adrienne Blair LITTLE a Yann BARTOSIEWICZ. A 1D model to predict ejector performance at critical and sub-critical operational regimes. *International Journal of Refrigeration* [online]. 2013, **36**(6), 1750–1761. ISSN 01407007. Dostupné z: doi:10.1016/j.ijrefrig.2013.04.009

[4] EXPÓSITO CARRILLO, J. A., F. J. SÁNCHEZ DE LA FLOR a J. M. SALMERÓN LISSÉN. Comparaison thermodynamique de cycles de refroidissement à éjecteur. Caractérisation d'éjecteur aux moyens du ratio d'entrainement et du rendement de compression. *International Journal of Refrigeration* [online]. 2017, **74**, 369–382. ISSN 01407007. Dostupné z: doi:10.1016/j.ijrefrig.2016.11.006

[5] BESAGNI, Giorgio, Riccardo MEREU a Fabio INZOLI. Ejector refrigeration: A comprehensive review. *Renewable and Sustainable Energy Reviews* [online]. 2016, **53**, 373–407. ISSN 18790690. Dostupné z: doi:10.1016/j.rser.2015.08.059

[6] SARKAR, Jahar. Ejector enhanced vapor compression refrigeration and heat pump systems—A review. *Renewable and Sustainable Energy Reviews*. 2012, **16**(9), 6647–6659. ISSN 1364-0321.

[7] RAHAMATHULLAH, Mohammed Raffe, Karthick PALANI a Prabakaran VENKATAKRISHNAN. A Review On Historical And Present Developments In Ejector Systems. *International Journal of Engineering Research and Applications (IJERA)*. 2013, **3**(2), 10–34.

[8]   SUMERU, K, H NASUTION a F N ANI. A review on two-phase ejector as an expansion device in vapor compression refrigeration cycle. *Renewable and Sustainable Energy Reviews*. 2012, **16**(7), 4927–4937. ISSN 1364-0321.

[9]   BANASIAK, Krzysztof a Armin HAFNER. 1D Computational model of a two-phase R744 ejector for expansion work recovery. *International Journal of Thermal Sciences*. 2011, **50**(11), 2235–2247. ISSN 1290-0729.

[10]   ŚMIERCIEW, Kamil, Jerzy GAGAN, Dariusz BUTRYMOWICZ a Jarosław KARWACKI. Experimental investigations of solar driven ejector air-conditioning system. *Energy and Buildings* [online]. 2014, **80**, 260–267. ISSN 03787788. Dostupné z: doi:10.1016/j.enbuild.2014.05.033

[11]   CHUNNANOND, Kanjanapon a Satha APHORNRATANA. Ejectors: applications in refrigeration technology. *Renewable and sustainable energy reviews*. 2004, **8**(2), 129–155. ISSN 1364-0321.

[12]   full-text. nedatováno.

[13]   The theory behind heat transfer [online]. nedatováno [vid. 2018-03-25]. Dostupné z: https://www.alfalaval.com/globalassets/documents/microsites/heating-and-cooling-hub/alfa_laval_heating_and_cooling_hub_the_theory_behind_heat_transfer.pdf

[14]   *What Are the Differences Between Pump Types?* [online]. [vid. 2018-03-25]. Dostupné z: https://www.globalpumps.com.au/blog/what-are-the-differences-between-pump-types

[15]   *World Leader in Triplex High Pressure Pumps* [online]. [vid. 2018-03-25]. Dostupné z: http://www.catpumps.com/products.asp?id=709&criteria=1

[16]   *» The Different Classifications Of Heat Exchangers* [online]. [vid. 2018-03-25]. Dostupné z: http://mahans.com/the-different-classifications-of-heat-exchangers/

[17]   *KAORI Brazed Plate Heat Exchanger BPHE - Kaori Heat Treatment Co., Ltd.Home* [online]. [vid. 2018-03-25]. Dostupné z: http://www.kaori-bphe.com/en/

[18]   *API Heat Transfer* [online]. [vid. 2018-03-25]. Dostupné z: http://www.apiheattransfer.com/

[19]   *Guide to Thermostatic Expansion Valves (TXV)* [online]. [vid. 2018-03-25]. Dostupné z: http://www.ac-heatingconnect.com/homeowners/guide-to-txv/

[20]   *Electronic expansion valves - ExV* [online]. [vid. 2018-03-25]. Dostupné z: http://www.carel.com/electronic-expansion-valve